Molecular Pharmacology Fast Forward. Published on March 17, 2011 as doi:10.1124/mol.110.069534

PTEN Inhibition by 4-Hydroxynonenal Leads to Increased Akt Activation in Hepatocytes

Colin T. Shearn, Rebecca L. Smathers, Benjamin J. Stewart, Kristofer S. Fritz, James J. Galligan, Numsen Hail Jr., and Dennis R. Petersen

Departments of Pharmaceutical Sciences (C.T.S., K.S.F., N.H. Jr., D.R.P.); Toxicology (R.L.S.); Pharmacology (J.J.G.); School of Pharmacy (C.T.S., R.L.S., K.S.F., N.H. Jr., D.R.P.); School of Medicine (J.J.G.), University of Colorado Denver, Aurora, Colorado. Center for Accelerator Mass Spectrometry (B.J.S.); Lawrence Livermore National Laboratory (B.J.S.), Livermore, California.

Molecular Pharmacology Fast Forward. Published on March 17, 2011 as DOI: 10.1124/mol.110.069534
This article has not been copyedited and formatted. The final version may differ from this version.

Running title: Inhibition of PTEN by 4-HNE

Corresponding Author: Dennis R. Petersen

Address: 12850 East Montview Blvd. V20-2232C, Aurora, CO. 80045.

Phone: 303-724-3397

Fax: 303-724-7266

E-mail: Dennis.Petersen@ucdenver.edu

Number of Text pages 33

Number of Tables 0

Number of references 39

Number of Words in Abstract 248

Number of words in Introduction 628

Number of words in Discussion 1289

Nonstandard abbreviation: 4-HNE, 4-hydroxynonenal, PTEN, phosphatase and tensin homolog deleted on chromosome 10, PtdIns (3,4,5) P_3, phosphatidylinositol (3,4,5) P_3, PI3K, phosphatidylinositol 3-kinase, PDK-1, phosphoinositide-dependent kinase 1, DCFDA, 2'7' dichlorofluorescein diacetate, PP2A, protein phosphatase 2A, PHLPP, pleckstrin homology domain leucine rich repeat protein phosphatases, O.A., okadaic acid

Molecular Pharmacology Fast Forward. Published on March 17, 2011 as DOI: 10.1124/mol.110.069534
This article has not been copyedited and formatted. The final version may differ from this version.

Abstract

The production of reactive aldehydes such as 4-hydroxynonenal (4-HNE) is proposed to be an important factor in the etiology of alcoholic liver disease. To understand the effects of 4-HNE on homeostatic signaling pathways in hepatocytes, cellular models consisting of the human hepatocellular carcinoma cell line (HepG2) and primary rat hepatocytes were evaluated. Treatment of both HepG2 cells and primary hepatocytes with subcytotoxic concentrations of 4-HNE resulted in the activation of Akt within 30 min as demonstrated by increased phosphorylation of residues Ser473 and Thr308. Quantification and subsequent immunocytochemistry of PtdIns (3,4,5) P_3 resulted in a 6 fold increase in total PtdIns (3,4,5) P_3 and increased immunostaining at the plasma membrane following 4-HNE treatment. Co-treatment of HepG2 cells with 4-HNE and the phosphatidylinositol 3-kinase inhibitor Ly294002 or the protein phosphatase 2A inhibitor okadaic acid, revealed that the mechanism of activation of Akt is PI3K-dependent and PP2A independent. Using biotin hydrazide detection, it was established that the incubation of HepG2 cells with 4-HNE resulted in increased carbonylation of the lipid phosphatase PTEN, a key regulator of Akt activation. Activity assays both in HepG2 cells and recombinant PTEN revealed a decrease in PTEN lipid phosphatase activity following 4-HNE application. Mass spectral analysis of 4-HNE treated recombinant PTEN detected a single 4-HNE adduct. Subsequent analysis of Akt dependent physiological consequences of 4-HNE in HepG2 cells revealed significant increases in the accumulation of neutral lipids. These results provide a potential mechanism of Akt activation and cellular consequences of 4-HNE in hepatocytes.

Molecular Pharmacology Fast Forward. Published on March 17, 2011 as DOI: 10.1124/mol.110.069534
This article has not been copyedited and formatted. The final version may differ from this version.

Introduction

Oxidative modification of proteins by reactive aldehydes has been implicated in an increasing number of hepatic disease states including hepatitis C, non-alcoholic steatohepatitis and chronic alcoholic liver disease (ALD) (Paradis et al., 1997; Roede et al., 2008; Seki et al., 2002). A documented marker for increased oxidative stress in cells is the presence of elevated levels of 4-hydroxynonenal (4-HNE). Reactive aldehydes such as 4-HNE originate from peroxidation of membrane lipids including linoleic acid (Poli et al., 2008). 4-HNE is a potent electrophile that will react with nucleophilic functional groups in DNA as well as Cys, Lys and His residues within proteins. Proteins documented to be targets for modification by 4-HNE include protein disulfide isomerase, actin, and thioredoxin (Carbone et al., 2005; Fang and Holmgren, 2006; Ozeki et al., 2005). Consistent with the potent electrophilic properties of 4-HNE, proteins modified by this biogenic aldehyde displayed compromised function.

Hepatocytes are well recognized for their ability to withstand oxidative stress associated with the production 4-HNE (Esterbauer et al., 1991). Previous studies have shown that hepatocytes metabolize 4-HNE to its glutathione conjugate which is then rapidly exported out of the cell. Treatment of rat H35 hepatoma cells with 25μM 4-HNE resulted in approximately 61% of the 4-HNE being converted to the glutathione adduct and exported out of the cells within 2-5 min (Tjalkens et al., 1999). In HepG2 cells, 4-HNE exposure at concentrations as high as 100μM for 2 h did not induce cell damage or death as indicated by changes in DNA or by LDH release (Stewart et al., 2009). In other studies using primary hepatocytes, 500μM 4-HNE was metabolized to the metabolites 4-hydroxynonenoic acid and 1,4-dihydroxynonene within 2 min (Hartley and Petersen, 1997).

The oncoprotein Akt is involved in the activation of cell survival pathways following oxidative insult. For example, in cells exposed to 1mM hydrogen peroxide, Akt is phosphorylated

Molecular Pharmacology Fast Forward. Published on March 17, 2011 as DOI: 10.1124/mol.110.069534
This article has not been copyedited and formatted. The final version may differ from this version.

on Thr308 and Ser473 leading to its complete activation resulting in increased cell survival. Under conditions of increased oxidative stress, Akt activation involves the oxidation and subsequent inactivation of PTEN (Leslie et al., 2003). As an initial step, Akt is recruited to the membrane by the association of its PH domain with phosphatidylinositol (3,4,5) trisphosphate (PtdIns (3,4,5) P_3). Once at the membrane, Akt is phosphorylated on Thr308 by phosphoinositide dependent kinase 1 (PDK1) followed by phosphorylation at Ser473 by mTORC2 (see ref (Liao and Hung, 2010) for comprehensive review).

The primary regulator of Akt is the tumor suppressor PTEN (phosphatase and tensin homolog deleted on chromosome 10). PTEN negatively regulates AKT activation via its lipid phosphatase activity (Di Cristofano and Pandolfi, 2000). PTEN is a phosphatidylinositol 3-phosphatase catalyzing the removal of the 3-position phosphate from PtdIns (3,4,5) P_3 to produce phosphatidylinositol (4,5) bisphosphate (PIP_2). PTEN is also susceptible to oxidative stress. Both ROS and reactive nitrogen species have been shown to modify and inactivate PTEN (Lee et al., 2002; Yu et al., 2005). Inactivation of PTEN leads to increased Akt activation in both cellular and animal models. In addition, hepatocyte specific deletion of PTEN leads to steatohepatitis and increased hepatocellular carcinoma in mice (Horie et al., 2004). Initiation of liver steatosis in these mice was linked with increased Akt activation and subsequent Akt dependent downstream activation of SREBP1c, PPARγ and Foxo1 (Watanabe et al., 2005).

In this communication, we describe the effects of 4-HNE on activation of Akt in a hepatocellular cell line as well as primary hepatocytes. Our results demonstrate that PTEN activity is inhibited following exposure to 4-HNE resulting in increased Akt activation as determined by increased Akt phosphorylation. Further, we demonstrate that the inhibition of PTEN coincides with adduction by 4-HNE. This report provides insight into the mechanisms of 4-HNE induced cellular signaling with respect to fatty acid production and liver injury induced by oxidative stress.

Molecular Pharmacology Fast Forward. Published on March 17, 2011 as DOI: 10.1124/mol.110.069534
This article has not been copyedited and formatted. The final version may differ from this version.

Materials and Methods

Preparation of recombinant PTEN (rPTEN)

Full-length rPTEN was amplified by PCR from pGEX4T-PTEN using the following oligonucleotides: PTEN-5' (5'-CCACATGACAGCCATCATCAAAGAG-3' sense) and PTEN-3' (5'-TCAGACTTTTGTAATTTGTGAATGC TG-3' antisense). Following amplification, the each fragment was TOPO-cloned into His-tagged pET100-TOPO (Invitrogen, Carlsbad, CA), transformed into TOP-10 cells and grown overnight on LB-ampicillin plates (100 μg/mL) according to the manufacturer's instructions. Colonies were picked and placed into 3-mL LB cultures for 16 h with 100 μg/mL of ampicillin. DNA was subsequently purified using Qiagen minipreps (Qiagen, Valencia, CA) and sequences were verified at the University of Colorado Cancer Center core facility. All oligonucleotides were purchased from IDT (Coralville, IA.)

To express the histidine-tagged rPTEN, rPTEN-pET100 DNA was transformed into BL-21 Star (DE3) *Escherichia coli*., colonies were picked and grown in 3 mL of LB plus 100 μg/mL ampicillin. After 16 h, 1mL of the culture was added to 100 mL of fresh LB broth together with ampicillin and the culture grown until it reached an OD_{600} of 0.8-1.0. The culture was then induced with 1 mM isopropyl-β-D-thiogalactopyranoside and grown for 4 h at 37 ^{o}C. Cultures were sedimented by centrifugation at 6,000 rpm for 20 min and flash frozen. For protein purification, pellets were thawed and cells lysed on ice for 20 min in 50 mM HEPES (pH 7.6), 300 mM NaCl, 10 mM imidazole, 2mM DTT, 0.5% Triton X-100, together with lysozyme and protease inhibitors (Sigma). This sample was sonicated with three 20 s bursts, followed by centrifugation at 14,000 rpm for 30 min. The supernatant was decanted and 150 μL of 50% immobilized nickel resin (Qiagen, Valencia, CA) in lysis buffer was added and the sample incubated for 4 h at 4^{o}C on a rotary mixer. Following incubation, the beads were washed five times with 50 mM HEPES (pH 7.6), 300 mM NaCl, containing 20 mM imidazole 2mM DTT,

Molecular Pharmacology Fast Forward. Published on March 17, 2011 as DOI: 10.1124/mol.110.069534
This article has not been copyedited and formatted. The final version may differ from this version.

then twice increasing to 50 mM imidazole, and finally eluted from the resin with 50 mM HEPES (pH 7.6), 300 mM NaCl, 150 mM imidazole and 10% glycerol 2mM DTT.

Cell culture

HepG2 cells were maintained at 50-80% confluence in RPMI supplemented with 10% Fetal Bovine Serum, 100mM Hepes, 100 IU/ml Penicillin, 100g/ml Streptomycin. Prior to each experiment, cells were plated into 6 well plates at a density of $1X10^6$ cells per well in RPMI plus serum and allowed to adhere overnight. The following day, the cells were washed twice in serum-free RPMI and treated with indicated doses of 4-HNE in serum-free media. Where indicated, Ly294002 (50μM preincubation/60 min) or okadaic acid (0.1μM preincubation/30 min) (Calbiochem/EMD, Gibbstown, NJ) were added with RPMI plus serum and also in the serum-free medium used for each 4-HNE treatment.

Western blotting

Cells were lysed for 5 min. in 50mM HEPES, 100mM NaCl, 1% triton X-100, 2mM EDTA pH 7.7 plus protease inhibitors SIGMA (St. Louis, MO), followed by sonication for 3X10 s and 20 μg loaded per well on 7% SDS PAGE gels, electroblotted to PVDF, blocked in Tris buffered saline with 1% Tween (TBST) and 5% nonfat dry milk for 1 h and incubated overnight in primary antibody. The following rabbit polyclonal primary antibodies were used at 1:1000 dilution in TBST: pSer473 Akt, p-Thr308 AKT, total Akt, p-PTEN (S380, T382, 383) and total PTEN (Cell Signaling #4691, 2965, 4060, 9549, 9552. Danvers, MA). The rabbit polyclonal 4-HNE antibody was used at 1:1000 as previously described (Stewart et al., 2007). The following morning blots were washed 3x5 min in TBST and incubated for 1 h in horseradish peroxidase conjugated goat polyclonal anti-rabbit secondary antibody (Jackson ImmunoResearch laboratories, West Grove, PA). Blots were washed 3x5 min in TBST and subsequently developed using chemiluminescence (Pierce Supersignal, Thermofisher Scientific, Rockford, IL) and developed on film.

Molecular Pharmacology Fast Forward. Published on March 17, 2011 as DOI: 10.1124/mol.110.069534
This article has not been copyedited and formatted. The final version may differ from this version.

Isolation of rat primary hepatocytes:

All animal procedures were approved by the Institutional Animal Care and Use Committee (IACUC) at the University of Colorado Denver Anschutz Medical Campus. Primary rat hepatocytes were isolated from the livers of untreated, laboratory chow-fed male Sprague-Dawley rats (~400 g) that were purchased from Jackson Laboratories (Bar Harbor, ME). The isolation procedure utilized a modified collagenase perfusion method. Hepatocytes were resuspended in RPMI 1640 media containing 10% fetal bovine serum (BSA) and penicillin/streptomycin (100 IU/ml and 100g/ml, respectively). Cell viability was assessed using Trypan blue exclusion, with viability exceeding 90%. Cells ($1x10^6$) were plated in 6-well plates coated with extracellular matrix (ECM) Gel from Engelbreth-Holm-Swarm murine sarcoma (Sigma Aldrich, St. Louis, MO), and allowed to acclimate to culture conditions at 37^oC + 5% CO_2 for 2 h before treatments.

Determination of ROS production

To determine the production of ROS within the cell a fluorescent indicator was used, (2'7' dichlorofluorescein diacetate (DCFDA). Cells in 6 well plates were washed twice in Krebs-Ringer buffer (KRB) solution followed by the addition of 20μM DCFDA and increasing concentrations of 4-HNE in KRB in triplicate wells for each treatment. The plates were then read at the dichlorofluorescein (DCF) emission wavelength of 538nm using a SpectraMax Gemini EM dual-scanning microplate spectrofluorimeter (Molecular Devices, Sunnyvale, CA). A time course reading every 5 min throughout a total of a 120 min period was evaluated. As a control, DCFDA and 4-HNE were also incubated in the absence of cells and no fluorescence was detected.

TR-FRET quantification of PtdIns (3,4,5) P3 in HepG2 cells.

$1X10^6$ cells were plated, allowed to adhere overnight and treated with either serum free media (Control) or 100μM 4-HNE in serum-free RPMI for 60 min. Cells were washed 2X in PBS and PtdIns (3,4,5)P_3 extracted as per PtdIns (3,4,5) P_3 Quantification

Molecular Pharmacology Fast Forward. Published on March 17, 2011 as DOI: 10.1124/mol.110.069534
This article has not been copyedited and formatted. The final version may differ from this version.

HTRF Assay kit (Millipore, Billerica, MA). Following extraction, extracted PtdIns (3,4,5)P_3 was placed in a 96-well-microtiter plate and the displacement of Biotinylated PtdIns (3,4,5)P_3 from a complex consisting of Europium labeled anti-GST antibodies, a GST-tagged PH domain, biotinylated PtdIns (3,4,5)P_3 and Streptavidin-Allophycocyanin (APC). The displacement of the biotinylated PtdIns (3,4,5)P_3 by extracted cellular PtdIns (3,4,5)P_3 resulted in a decrease in the fluorescent emission of Europium complex following excitation at 330nm and emission 620nm and 665nm. All plates were read on a BioTek Synergy 4 Hybrid Multi-Mode Microplate reader (BioTek Instruments, Winooski, Vt). Concentrations of PtdIns (3,4,5)P_3 were obtained by plotting the ratio of E_{665}/E_{620} multiplied by 10,000 using GraphPad PRISM 4 as per the manufacturer's instructions.

Adduction of recombinant PTEN by 4-HNE

Two µg of rPTEN was treated with 4-HNE at molar ratios of 1:1 and 10:1 for 30 min at 37^{o}C. Samples were then boiled in 5X SDS loading buffer, run on a 7.5% SDS PAGE gel and Western blotted using anti-4-HNE polyclonal antibodies. To verify PTEN adduction, membranes were then stripped for 15 min using stripping buffer (Pierce, Rockford, IL), washed twice in TBST and blocked once again for 1 h in TBST 5% NFDM. Following blocking, membranes were incubated overnight with mouse anti-PTEN (Cell Signaling #9556) and subsequently processed.

Biotin hydrazide modification of carbonylated PTEN

To determine reactive aldehyde adduction, 1X10^7 HepG2 cells were treated with 100µM 4-HNE for 1 h in serum free media. Cells were then lysed in 50mM HEPES, 100mM NaCl, 2mM EDTA, 2.5mM biotin hydrazide and allowed to incubate for 30 minutes at RT. To remove excess biotin, lysates were dialyzed overnight at 4^{o}C. Biotinylated proteins were pulled down incubating

Molecular Pharmacology Fast Forward. Published on March 17, 2011 as DOI: 10.1124/mol.110.069534
This article has not been copyedited and formatted. The final version may differ from this version.

with streptavidin agarose beads (Pierce) on a rotary mixer at 4°C for 3h, washed five times in PBS and loaded onto SDS PAGE gels and processed according to western blotting protocols.

In vitro PTEN activity assay

To assess activity of recombinant untreated and 4-HNE treated PTEN, a phosphate release assay was used with Biomol Green as an indicator. For each assay, 2 µg of rPTEN was incubated for 30 min at RT with increasing molar amounts of 4-HNE in 50mM Tricine, 100mM NaCl (pH 8.0). Unreacted 4-HNE was quenched using 2mM DTT for 30 min at room temperature. Phosphatase assays were performed in 50µl of reaction buffer, 200µM water-soluble DiC_8-PtdIns (3,4,5)P_3 (Echelon, Salt Lake City, UT) for 40 min at 37°C. The reactions were stopped and the released phosphate measured by incubating the samples for 20 min with 200µl of Biomol Green (Biomol, Plymouth Meeting, PA). Following incubation, samples were read using a microtiter plate reader at 620nm on a SpectraMax 190 microplate spectrofluorimeter (Molecular Devices, Sunnyvale, CA). Values were determined as nmol PtdIns (3,4,5)P_3 released per min and subsequently converted to percent of control reactions.

MS analysis of 4-HNE modified recombinant PTEN

4-HNE exposed human rPTEN (Cayman Chemical) was examined to determine if protein adduction occurred *in vitro*. Briefly, 2.4 µg (0.05 nmoles) of rPTEN was incubated with a 5x molar excess of 4-HNE (0.25 nmoles) for 30 min at 25°C. The control and treated samples were concentrated using C18 ZipTips (Millipore, Billerica, MA), mixed 1:1 with sinapinic acid (SA, 10 mg/mL) and spotted in 1 µl aliquots onto an Opti-TOF 96 well insert (Applied Biosystems, Foster City, CA). An ABI 4800 Plus MALDI-TOF mass spectrometer (Applied Biosystems) was used to characterize the adduction of rPTEN by 4-HNE. The instrument was operated under standard conditions for intact protein at a laser power of 5500 and was calibrated using the 1+ and 2+ charge states of bovine serum albumin. MS analysis was performed using standard Linear

Molecular Pharmacology Fast Forward. Published on March 17, 2011 as DOI: 10.1124/mol.110.069534
This article has not been copyedited and formatted. The final version may differ from this version.

High Mass acquisition and processing methods with a focus mass of 50 kDa. Data analysis was performed using Applied Biosystems' 4000 Series Explorer v 3.5.

Cellular PTEN activity assay

Following treatment, HepG2 cells were lysed in 50mM HEPES, 100mM NaCl, 1% tritonX-100, 2mM EDTA plus protease inhibitors. Lysates were subsequently precleared with Protein A agarose (Sigma Aldrich, Saint Louis, MO) beads for 1 h. To the cleared lysates, fresh Protein A agarose and 2µg of rabbit polyclonal anti-PTEN was added and the samples incubated on a rotomixer overnight at 4^{o}C. Samples were washed four times in lysis buffer and activity assays performed as per *in vitro* protocol with the exception of incubation with substrate was for 30 min on a rotary mixer. Beads were separated by centrifugation at 1000xg and supernatants placed in 96 well microtiter plates. Phosphate release was measured using Biomol Green as previously described.

Nile red staining and confocal microscopy

HepG2 cells were grown on glass cover slips and treated with 4-HNE or colchicine for 1 h, and allowed to recover for 24 hrs. Cells were fixed with 10% neutral buffered formalin for 30 min at room temperature, and the cover slips were then extracted for 20 min at room temperature with PBS, pH 7.4, containing 2.5% bovine serum albumin (BSA) and 1% Triton X-100. Cover slips were then washed three times for 5 min with TBS. For Nile red neutral lipid staining, after fixation, extraction, and washing, cover slips were incubated with 20 µg/mL Nile Red in TBS for 30 min, and washed once in TBS and mounted with DAPI-containing mounting medium DAPI (Vector Laboratories, Burlingame, CA). Confocal images were taken with a 100X oil immersion objective on a Nikon Eclipse TE2000-E instrument, with identical instrument laser and contrast settings used within each group. Images were acquired using EZ-C1 software (Nikon, Melville, NY).

Nile red cellular neutral lipid accumulation assay and cellular DNA measurement

Molecular Pharmacology Fast Forward. Published on March 17, 2011 as DOI: 10.1124/mol.110.069534
This article has not been copyedited and formatted. The final version may differ from this version.

HepG2 cells were grown on 6-well plates to greater than 90% confluence and were treated for 1 h with 4-HNE, brefeldin a, diethylmaleate (DEM), oleic acid conjugated to BSA, or colchicine, followed by a 24 h recovery in serum-containing RPMI 1640 media. Nile red was used to detect cellular neutral lipid using a modification of previously reported techniques, and Hoechst 33342 was used to measure cellular DNA (McMillian et al., 2001). Cells were collected in 1 mL of phenol red-free, serum-free RPMI 1640, and 50 µL of cell suspension was incubated in sterile 96 well fluorescence plates for 1 hour at 37° C with 200 µL of serum-free, phenol red-free RPMI 1640 containing Nile Red at 20 µg/mL and Hoechst 33342 at 10 µg/mL. Plates were shaken for 10 seconds prior to reading, and neutral lipid was assessed by Nile red fluorescence with excitation 485nm/ emission 565 nm, and was normalized against cellular DNA as measured by Hoechst 33342 staining measured with excitation 355 nm/ emission 465 nm.

Immunocytochemical analysis of PtdIns (3,4,5) P_3 in HepG2 cells using Confocal microscopy.

$2X10^5$ HepG2 cells were plated on cover slips in 6-well plates for 24hr in RPMI + 10% serum. The following morning cells were washed 2X in serum free RPMI and treated with 100µM 4-HNE (60min) or 100nM insulin (30min). Following treatment, cells were washed 1X in PBS and fixed in 3.7% paraformaldehyde in PBS for 30 min. Following fixation, cells were washed 1X in PBS and permeabilized using 0.15% tritonX100 in PBS for 10 min. Cells were then incubated for 1hr in RPMI plus 10% bovine serum (blocking reagent) washed 2X in PBS and incubated overnight in mouse monoclonal anti-PtdIns (3,4,5) P_3 (Echelon Biosciences, Salt Lake City, UT) with RPMI 2% bovine serum. Plates were washed 3X10 min in PBS followed by incubation for 60 min in Texas red conjugated goat anti-mouse secondary antibody (Molecular Probes, Eugene, OR). Cover slips were washed 2X in PBS, mounted using Vectastain mounting media (Vector Labs, Burlingame, CA) with 10 µg/mL Hoechst 33342 (SIGMA):Supermount (Biogenex, San Ramon, CA)(1:4) and allowed to dry at 4^oC overnight. Slides were then analyzed using Confocal

Molecular Pharmacology Fast Forward. Published on March 17, 2011 as DOI: 10.1124/mol.110.069534
This article has not been copyedited and formatted. The final version may differ from this version.

microscopy, Texas red fluorescence (excitation 485nm/ emission 565 nm) Hoechst 33342 staining (excitation 355 nm/ emission 465 nm).

Confocal microscopy of GFP-TAPP1 localization in HepG2 cells.

$2X10^7$ HepG2 cells were electroporated with 30µg of GFP-TAPP1 (A kind gift from Dr. A.J. Marshall, University of Manitoba, Canada) or eGFP control in 200 microliters of PBS (without Ca^{2+}or Mg^{+}) using a Biorad Gene Pulsar at 960µF, 300V, 29µsec. $2X10^5$ cells were subsequently plated into 6 well plates containing coverslips and allowed to adhere overnight. Cells were washed 2X in serum free RPMI and treated with 100µM 4-HNE (60min) or 100nM insulin (30min). Following treatment, cells were washed 2X in PBS and mounted using Vectastain mounting media with 10 µg/mL Hoechst 33342 and allowed to dry at 4^oC overnight. Slides were then analyzed using Confocal microscopy-GFP (excitation 395nm/ emission 488nm) Hoechst 33342 staining (excitation 355 nm/ emission 465 nm).

Statistical analysis

Relative densitometry of Western blots was quantified using ImageJ (NIH). All data and statistic analysis was performed using 1-way ANOVA and Graph Pad Prism IV for Windows (Graph Pad Inc. La Jolla, CA). All data are expressed as mean +/- standard error and p values<0.05 were considered significant.

Molecular Pharmacology Fast Forward. Published on March 17, 2011 as DOI: 10.1124/mol.110.069534
This article has not been copyedited and formatted. The final version may differ from this version.

Results

4-HNE activates Akt via a concentration dependent mechanism.

The PTEN/Akt pathway has been implicated in increased cell survival following cellular stress (Lee et al., 2002; Yu et al., 2005). Full activation of Akt requires sequential phosphorylation on both Thr308 and Ser473 (Liao and Hung, 2010). To evaluate the effect of 4-HNE on Akt in HepG2 cells, cells were exposed to increasing concentrations of 4-HNE (0-100μM) for 60 min in serum free media (Figure 1A). As a positive control, 1mM H_2O_2 (5 min) was added. Cells were subsequently lysed and Western blots probed for increased levels of phosphorylation on Ser473 and Thr308 of Akt. It is apparent from Figure 1A, that Akt is not phosphorylated in control samples whereas both Ser473 and Thr308 are phosphorylated at concentrations of 4-HNE ranging from 25-100μM.

To further explore the time course of Akt activation, a time course (0-120 min) was performed using 100μM 4-HNE in serum free media (Figure 1B). As expected, in the untreated controls, removal of serum for 2 h showed a progressive decrease in Akt phosphorylation in the control. 4-HNE, however, led to an initial decrease in Akt phosphorylation within 5 min followed by an increase in phosphorylation by the 30 min time point extending to 120 min. Densitometric analysis indicated that Akt phosphorylation at Ser473 peaks at 60 min with a statistically significant decrease by 120 min (Figure 1C). Overall, these data demonstrate a concentration-dependent, time-dependent activation of Akt following 4-HNE treatment.

ROS is a known regulator of Akt activation and 4-HNE has been linked to increased reactive oxidative species (ROS) production in certain cell types (Go et al., 2007; Raza and John, 2006). To dissociate ROS mediated Akt activation from 4-HNE, cells were treated with increasing doses of 4-HNE in serum free media and examined for the oxidation of 2'7' dichlorofluorescin to DCF over a 120 min period. From Figure 2, incubation of HepG2 cells with concentrations of 4-HNE below 250μM led to a decrease in the rate of ROS generation as

Molecular Pharmacology Fast Forward. Published on March 17, 2011 as DOI: 10.1124/mol.110.069534
This article has not been copyedited and formatted. The final version may differ from this version.

detected via the oxidation of DCFDA compared to untreated cells. As a positive control for this assay, 1mM hydrogen peroxide led to a dramatic short-term increase in DCF production suggestive of enhanced ROS production. To establish that lack of ROS production was dependent on the time of exposure to 4-HNE, a time course was also performed over 2 h in serum free media. Similar rates of ROS production occurred throughout the time course (Data not shown). These data suggest an ROS-independent mechanism of Akt activation by 4-HNE.

Effects of 4-HNE on PtdIns (3,4,5) P_3 and PtdIns (3,4) P_2 in HepG2 cells.

Previous biochemical studies have shown stimulation of Akt activation requires production of PtdIns (3,4,5) P_3 or PtdIns (3,4) P_2 (Liao and Hung, 2010). To examine the effects of 4-HNE on overall concentrations of PtdIns (3,4,5) P_3, time-resolved fluorescence resonance energy transfer (TR-FRET) was used. The data presented in Figure 3A demonstrate a 6 fold increase in cellular PtdIns (3,4,5) P_3 concentrations following 4-HNE treatment. To further characterize changes in intracellular PtdIns (3,4,5) P_3, confocal microscopy and immunocytochemistry was performed using anti-PtdIns (3,4,5) P_3 antibodies. In Figure 3B, compared to control cells, increased PtdIns (3,4,5) P_3 staining is evident at the plasma membrane (arrows) in both the 4-HNE treated and insulin treated cells.

The phosphatidylinositol binding protein tandem-PH-domain-containing protein-1 (TAPP1) binds specifically to PtdIns (3,4) P_2 and has been shown to be regulated by insulin (Marshall et al., 2002; Wullschleger et al.). To gain a better understanding of the intracellular effects of 4-HNE on PtdIns (3,4) P_2, GFP-tagged TAPP1 domain (Figure 3C) or eGFP (Supplemental Figure 1) alone was overexpressed in HepG2 cells. After 24 hrs, cells were stimulated with either 4-HNE (100μM, 60 min) or insulin (100nM, 30 min) in serum free media and examined using confocal microscopy. From Supplemental Figure 1, both 4-HNE and insulin had no effect of localization of eGFP. In Figure 3C, GFP-TAPP1 localization is primarily cytosolic in unstimulated cells. Surprisingly, 4-HNE did not have an effect on TAPP1

Molecular Pharmacology Fast Forward. Published on March 17, 2011 as DOI: 10.1124/mol.110.069534
This article has not been copyedited and formatted. The final version may differ from this version.

localization; insulin however, showed a mild increase in plasma membrane accumulation of GFP-TAPP1 (arrows). Combined these data suggest 4-HNE treatment leads to an increase in PtdIns (3,4,5) P_3 production but not an increase in PtdIns (3,4) P_2 production.

Activation of Akt by 4-HNE is PtdIns (3,4,5)P_3 dependent.

Full activation of Akt requires phosphorylation of Thr308 and Ser473. To further understand the mechanism of Akt activation following 4-HNE treatment, HepG2 cells were incubated with either a PI3K inhibitor (Ly294002) (Figure 4A) or a protein phosphatase 2A inhibitor (PP2A) (okadaic acid (O.A.)) (Figure 4B, short exposure, Supplemental Figure 2-long exposure). It is evident from Figure 4A, that Akt activation was significantly reduced following pre-incubation of Ly294002. Quantification and statistical analysis of Figure 4A indicate a statistically significant (95%) reduction in Ser473 phosphorylation following Ly294002 incubation (Figure 4C). These data suggest a PI3K-dependent mechanism of Akt activation by 4-HNE. In Figure 4B, pre-incubation with okadaic acid increased phosphorylation of Thr308 in both the control cells and the 4-HNE-treated cells. Although no change in phosphorylation of Thr308 is evident in the control lanes in Figure 4B, a longer exposure using the same samples clearly indicates an increase in phosphorylation in the control plus O.A. samples (Supplemental Figure 2). Figure 4D represents the quantification of the Western blots in Figure 4B, Supplemental Figure 2. A comparison of the control samples and the 4-HNE treated samples indicated a similar 2-fold change in both the control/control O.A. and the 4-HNE/4-HNE O.A. samples.

The dephosphorylation of Akt on Ser473 has been determined to not be a substrate of PP2A, but is a substrate of PHLPP. Therefore, okadaic acid should have no effect on Ser473 phosphorylation (Liao and Hung, 2010). There was no change in phosphorylation on Ser473 following O.A. treatment of 4-HNE treated cells (Supplemental Figure 3A). Although no inhibitors of PHLPP are available, total levels were examined by Western blot and no significant changes in protein expression were seen (Supplemental Data Figure 3B). As previously

Molecular Pharmacology Fast Forward. Published on March 17, 2011 as DOI: 10.1124/mol.110.069534
This article has not been copyedited and formatted. The final version may differ from this version.

mentioned, Akt is phosphorylated at Thr308 by PDK1 which is thought to be a constitutively active enzyme that also is recruited to the membrane by a PtdIns (3,4,5) P_3 dependent mechanism (Bayascas, 2008). 4-HNE had no effect on phosphorylation of PDK1 or total levels of PDK1 in HepG2 cells (Supplemental Data Figure 3B). Collectively, these data suggest that Akt activation occurs via a PI3K dependent mechanism and is not dependent on the inactivation of Akt specific protein phosphatases.

PTEN phosphorylation is decreased following 4-HNE exposure.

In cells, PTEN serves as a negative regulator of Akt by dephosphorylating the PI3K product PtdIns (3,4,5) P_3. Regulation of PTEN occurs via phosphorylation of C-terminal residues Ser380/Thr382/383 leading to an inactive state (Vazquez et al., 2001). To determine if 4-HNE affected the phosphorylation state of the C-terminus of PTEN, HepG2 cells were exposed to 100μM 4-HNE for a time course of 5-120 minutes (Figure 5A). Surprisingly, a time-dependent dephosphorylation occurs on the C-terminus of PTEN following 4-HNE treatment. The change in phosphorylation is also associated with an increase in the overall migration of PTEN (Figure 5A). To further explore the phospho-status of PTEN, HepG2 cells were pretreated with okadaic acid, lysed and the phospho-status of PTEN examined. No change in PTEN phosphorylation was evident following PP2A inhibition (Data not shown).

In cells, C-terminal dephosphorylation activates PTEN leading to decreased Akt activation (Vazquez et al., 2001). This is contrary to what is actually observed in our model. To determine the effects of 4-HNE on PTEN activity in HepG2 cells, PTEN activity assays were performed using immunoprecipitated PTEN from 4-HNE treated HepG2 cells. As a positive control, 1mM hydrogen peroxide was used to verify PTEN inhibition (Lee et al., 2002; Leslie et al., 2003). From Figure 5B, at the 25μM 4-HNE concentration, PTEN activity decreased 50% compared to control suggesting that although PTEN is dephosphorylated, activity is inhibited by

Molecular Pharmacology Fast Forward. Published on March 17, 2011 as DOI: 10.1124/mol.110.069534
This article has not been copyedited and formatted. The final version may differ from this version.

4-HNE. Thus, the decrease in overall PTEN activity, in addition to the decrease in PTEN phosphorylation, suggests an alternative mechanism of regulation of this phosphatase.

PTEN is carbonylated following 4-HNE treatment in HepG2 cells

To determine if cellular PTEN is adducted by 4-HNE, a method of biotin hydrazide modification of protein bound reactive aldehydes was employed (Figure 6A) (Grimsrud et al., 2007). HepG2 cells were exposed to 100μM 4-HNE, treated with 2.5mM biotin hydrazide and purified using streptavidin beads. Western blot analysis of streptavidin pull-downs indicates an increase in PTEN carbonylation (reactive aldehyde modification) following 4-HNE exposure. Subsequent quantification of the Western blots demonstrates a 2.5 fold increase in aldehyde modified PTEN in 4-HNE treated cells as compared to controls (Figure 6B). Overall, these data demonstrate intracellular carbonylation of PTEN readily occurs as a consequence of exposure to physiologically relevant concentrations of 4-HNE.

Characterization of PTEN modification by 4-HNE in vitro

To further examine the effects of 4-HNE on PTEN activity, recombinant PTEN (rPTEN) was treated with increasing molar ratios of 4-HNE followed by Western blotting using 4-HNE specific polyclonal antibodies and PTEN PtdIns (3,4,5)P_3 activity assays. The data presented in Figure 7A demonstrate that rPTEN is modified by 4-HNE at a concentration of 0.25μM which is equivalent to a molar ratio of 1:1. The data in Figure 7B demonstrate that PTEN is susceptible to inactivation by 4-HNE with an estimated IC_{50} of 1.5μM. This value corresponds to a molar ratio of approximately 2.5-5:1 moles of 4-HNE per mole of rPTEN consistent with the cellular data demonstrating PTEN modification and inhibition by 4-HNE (Figure 6). To further substantiate the ability of 4-HNE to modify PTEN MALDI-TOF mass spectrometry was performed. The MALDI-TOF mass spectrometry data presented in Figure 8 confirm modification of PTEN by 4-HNE. Following 4-HNE modification at a molar ratio of 5:1, a mass shift of 156Da was detected corresponding to the Michael-addition of 1 mole of 4-HNE to rPTEN.

Molecular Pharmacology Fast Forward. Published on March 17, 2011 as DOI: 10.1124/mol.110.069534
This article has not been copyedited and formatted. The final version may differ from this version.

Effects of 4-HNE on lipid accumulation

Previous reports have suggested a link between increased hepatic oxidative stress and lipid accumulation (Grattagliano et al., 2008; Sorrentino et al.). We therefore sought to characterize the effects of reactive aldehydes generated as a result of oxidative stress on cellular neutral lipid accumulation by HepG2 cells. Following a 1 h. exposure to 100μM 4-HNE and a 24 hr. recovery period, a significant increase ($p<0.01$) in cellular neutral lipid was observed (Figure 9A). Confocal microscopy experiments, using Nile red staining of cellular lipids, confirmed an increase due to 4-HNE treatment, while colchicine treatments were not discernibly different from control cells (Figure 9B). Because microtubule disruption (colchicine) and Golgi complex disruption (brefeldin a) impair export of lipids from hepatocytes, cellular lipid accumulation was measured following treatment with these compounds as well as with the glutathione-depleting agent diethyl maleate (DEM) (Figure 9C). These treatments failed to alter cellular neutral lipid content, while oleic acid conjugated to bovine serum albumin dramatically increased cellular lipid accumulation. Taken together, these results demonstrate 4-HNE-dependent increases in lipid accumulation in HepG2 cells.

Akt is activated by 4-HNE in primary hepatocytes

All of the previous experiments were performed in the HepG2 hepatocellular carcinoma cell line. To verify that Akt is also activated following 4-HNE treatment in primary cells, primary rat hepatocytes were isolated, plated on matrigel and experiments performed using increasing concentrations of 4-HNE (0-100μM). The dose-response experiments presented in Figure 10A demonstrate Akt phosphorylation following exposure to 100μM 4-HNE consistent with Figure 1A. The data presented in Figure 10B clearly indicates a statistically significant increase in phosphorylation of Akt on Ser473 following treatment of both 50 μM 4-HNE (2 fold) and 100μM 4-HNE (4 fold) for 1 hr. In agreement with the dose response, data presented in Supplemental Figure 5 demonstrate time-dependent 4-HNE mediated Akt phosphorylation in primary

Molecular Pharmacology Fast Forward. Published on March 17, 2011 as DOI: 10.1124/mol.110.069534
This article has not been copyedited and formatted. The final version may differ from this version.

hepatocytes is similar to that observed in HepG2 cells (Figure 1B). Combined, these data confirm 4-HNE activates Akt both in HepG2 cells and in primary hepatocytes.

Molecular Pharmacology Fast Forward. Published on March 17, 2011 as DOI: 10.1124/mol.110.069534
This article has not been copyedited and formatted. The final version may differ from this version.

Discussion

Chronic liver diseases affect a large percentage of the population today. These diseases include nonalcoholic steatohepatitis and the pathogenic effects of chronic alcoholism (Roede et al., 2008; Seki et al., 2002). A common factor in many of these diseases is their association with oxidative stress and dysregulation of lipid homeostasis. The widely recognized biomarker of oxidative stress, 4-HNE, is documented to have a number of bioactivities including covalent modification of protein and DNA which contribute to increased rates of mutation and altered protein function (Poli et al., 2008). Therefore, understanding the interaction of 4-HNE with cellular pathways and their subsequent mechanisms of activation/inactivation is essential to understanding the pathogenesis of chronic diseases associated with oxidative stress. In this report we characterize the mechanisms of Akt modulation by 4-HNE HepG2 cells and primary hepatocytes.

Previous studies have demonstrated the ability of ROS to activate Akt via PTEN oxidation (Lee et al., 2002; Leslie et al., 2003). In U87MG cells, 1mM H_2O_2 resulted in increased PtdIns (3,4,5) P_3 levels due to oxidation and inactivation of PTEN. PTEN null-cells did not exhibit the same increase (Leslie et al., 2003). 4-HNE has been shown to lead to increased production of intracellular ROS in aortic endothelial cells as determined by Dichlorofluorescein fluorescence (Go et al., 2007). In Figure 2 of the present study, treatment of 4-HNE did not lead to the increased production of ROS in HepG2 cells. The absence of measurable ROS suggests 4-HNE-specific effects of Akt activation.

Hepatocytes have previously been reported more resistant to 4-HNE mediated cellular toxicity than other cell types. Previous reports have suggested that Akt is either activated or inactivated following treatment with 4-HNE in other cell lines. In Jurkat T-cells, Akt is downregulated following 4-HNE exposure under serum free conditions (Liu et al., 2003). However, these cells have a deletion of PTEN leading to constitutively activated Akt, which could lead to discrepancies in Akt signaling following 4-HNE treatment (Shan et al., 2000). In

Molecular Pharmacology Fast Forward. Published on March 17, 2011 as DOI: 10.1124/mol.110.069534
This article has not been copyedited and formatted. The final version may differ from this version.

neuroblastoma cells, Akt is phosphorylated and activated in response to 4-HNE, yet these experiments were performed in the presence of serum (Dozza et al., 2004). Growth factors in serum are known to activate Akt, which could lead to undesirable complications such as variation in actual concentration and inadvertent activation via growth factor stimulation.

To determine direct effects of 4-HNE on the activation of Akt, 4-HNE was added in the absence of serum. In primary hepatocytes and in HepG2 cells we demonstrate that there is a corresponding increase in Akt phosphorylation that is both concentration and time dependent, reflecting activation of Akt by 4-HNE (Figure 1A-C, Figure 10A and B and Supplemental Figure 5). It should be noted that higher concentrations were required to induce a significant change in phosphorylation in the primary cells when compared to the hepatocellular carcinoma cells. This discrepancy could be due to several possibilities, the first being that primary hepatocytes metabolize 4-HNE more effectively due to increased amounts of 4-HNE metabolizing enzymes such as alcohol dehydrogenase which is lacking in HepG2 cells (Hartley et al., 1995).

As previously mentioned, Akt is regulated by protein phosphorylation/dephosphorylation mechanisms. Protein phosphatases such as PP2A have previously been shown to be activated by 4-HNE and dephosphorylate Akt in Jurkat cells leading to apoptosis (Liu et al., 2003). It is quite possible that PP2A activity is regulated by 4-HNE in hepatocytes. To examine the relative contribution of PP2A, an inhibitor was used. Okadaic acid led to a 2-fold increase in both the control and the 4-HNE treated cells (Figure 4B, Supplemental Figure 2). This indicates that PP2A inhibition does not significantly contribute to the increase in Akt phosphorylation following 4-HNE. To become active, Akt is recruited to the membrane via PtdIns (3,4,5) P_3. The data in Figure 2A and 2B demonstrate 4-HNE treatment leads to an increase in PtdIns (3,4,5) P_3 at the plasma membrane. In addition, in Figure 4A, in the presence of a PI3K inhibitor, 4-HNE inhibited Akt phosphorylation. Combined, these data suggest that 4-HNE-dependent Akt activation is due to increased levels of PtdIns (3,4,5) P_3 and not due to PP2A regulation.

Molecular Pharmacology Fast Forward. Published on March 17, 2011 as DOI: 10.1124/mol.110.069534
This article has not been copyedited and formatted. The final version may differ from this version.

By regulating PtdIns (3,4,5) P_3 levels in cells, PTEN is a direct regulator of Akt activation. PTEN is also regulated by phosphorylation. Increased phosphorylation of Ser380, Thr382/383 in the c-terminus of PTEN decreases PTEN stability and activity (Cho et al., 2004; Lee et al., 2002; Leslie et al., 2003; Yu et al., 2005). To determine if PTEN is regulated by phosphorylation, Western blotting was performed using PTEN phospho-specific antibodies. Based on the observed decrease in PTEN phosphorylation in Figure 4A Akt should be not be phosphorylated. However, in this system Akt is phosphorylated, suggesting that PTEN phosphorylation does not play a role in Akt activation in this system.

PTEN has also been shown to be regulated by direct modification of its active site cysteine. The pKa of the active site cysteine in PTEN (Cys124) is approximately 4.8, making it a very good nucleophile and target for 4-HNE modification (Lee et al., 2002; Leslie et al., 2003). Using Streptavidin purification of biotin hydrazide modified PTEN and MALDI-TOF MS, the data presented in Figures 6 and 8 verify that PTEN is a novel target of 4-HNE within the cell and *in vitro*. In addition, PTEN lipid phosphatase assays presented in Figure 5B demonstrate 4-HNE mediated PTEN inhibition in HepG2 cells. Furthermore, as shown in Figure 6A and B, direct modification of recombinant PTEN by 4-HNE leads to inhibition of enzyme activity at low micromolar concentrations. Combined, these data provide a potential mechanism for Akt activation by 4-HNE. It should be stressed that these concentrations of 4-HNE are well within the physiologic range in cells undergoing lipid peroxidation. Concentrations of 4-HNE within membranes have been calculated to be between 3.8 and 100mM (Benedetti et al., 1984) and low micromolar concentrations of 4-HNE are known to occur during chronic sustained oxidative stress (Esterbauer et al., 1991; Tsukamoto et al., 1995).

The PTEN/Akt pathway is an important regulator of cell survival and fatty acid metabolism. Hepatospecific deletion of PTEN leads to increased steatosis via upregulation of Akt (Horie et al., 2004). Deletion studies of both PTEN and Akt2, or Akt2 alone, demonstrated the necessity of the PTEN/Akt pathway in hepatic lipid accumulation (He et al., 2010; Leavens et al.,

Molecular Pharmacology Fast Forward. Published on March 17, 2011 as DOI: 10.1124/mol.110.069534
This article has not been copyedited and formatted. The final version may differ from this version.

2009). Accumulation of liver triglycerides was significantly decreased in the PTEN$^{-/-}$/Akt2$^{-/-}$ mice when compared to PTEN$^{-/-}$ mice (He et al., 2010). Although modest, this report demonstrates a significant increase in lipid accumulation 24 hours after 4-HNE addition to hepatocytes. Lipid accumulation could occur via Akt dependent biosynthetic pathways or it could be due to defects in lipid transport/β-oxidation. The activation of Akt by PTEN inhibition provides at least a partial mechanism for lipid increases exhibited following 4-HNE treatment.

4-HNE is an established biomarker for increased levels of oxidative stress in many chronic inflammatory diseases. Concentrations of 4-HNE within the cell have been estimated to be between 10μM (cytosolic) to greater than 3.8mM (membrane) (Benedetti et al., 1984; Tsukamoto et al., 1995). PTEN is known to associate with membranes via its C2 domain placing it in an ideal position for interaction with 4-HNE (Lee et al., 1999). In this study, we find that treatment of HepG2 cells and primary rat hepatocytes with 4-HNE leads to increased Akt activation as seen by increased phosphorylation at Ser473 and Thr308. Collectively, these experiments demonstrate a significant increase of 4-HNE-dependent fatty acid accumulation in HepG2 cells. The mechanism of Akt activation by 4-HNE is likely due to direct modification of PTEN by 4-HNE leading to inhibition of lipid phosphatase activity (Scheme 1). Akt activation during chronic inflammation *in vivo*, may partially be due to 4-HNE mediated PTEN inhibition, further contributing to increased steatosis in both non-alcoholic steatohepatitis and chronic ethanol models.

Molecular Pharmacology Fast Forward. Published on March 17, 2011 as DOI: 10.1124/mol.110.069534
This article has not been copyedited and formatted. The final version may differ from this version.

Authorship Contribution

Participated in research design: Shearn, Stewart

Conducted experiments: Shearn, Stewart, Fritz

Contributed new reagents or analytic tools: Smathers, Hail

Wrote or contributed to the writing of the manuscript: Shearn, Stewart, Fritz, Smathers, Galligan.

Molecular Pharmacology Fast Forward. Published on March 17, 2011 as DOI: 10.1124/mol.110.069534
This article has not been copyedited and formatted. The final version may differ from this version.

References

Bayascas JR (2008) Dissecting the role of the 3-phosphoinositide-dependent protein kinase-1 (PDK1) signalling pathways. *Cell Cycle* **7**(19):2978-2982.

Benedetti A, Comporti M, Fulceri R and Esterbauer H (1984) Cytotoxic aldehydes originating from the peroxidation of liver microsomal lipids. Identification of 4,5-dihydroxydecenal. *Biochim Biophys Acta* **792**(2):172-181.

Carbone DL, Doorn JA, Kiebler Z and Petersen DR (2005) Cysteine modification by lipid peroxidation products inhibits protein disulfide isomerase. *Chem Res Toxicol* **18**(8):1324-1331.

Cho SH, Lee CH, Ahn Y, Kim H, Ahn CY, Yang KS and Lee SR (2004) Redox regulation of PTEN and protein tyrosine phosphatases in H(2)O(2) mediated cell signaling. *FEBS Lett* **560**(1-3):7-13.

Di Cristofano A and Pandolfi PP (2000) The Multiple Roles of PTEN in tumor Suppression. *Cell* **100**:387-390.

Dozza B, Smith MA, Perry G, Tabaton M and Strocchi P (2004) Regulation of glycogen synthase kinase-3beta by products of lipid peroxidation in human neuroblastoma cells. *J Neurochem* **89**(5):1224-1232.

Esterbauer H, Schaur RJ and Zollner H (1991) Chemistry and biochemistry of 4-hydroxynonenal, malonaldehyde and related aldehydes. *Free Radic Biol Med* **11**(1):81-128.

Fang J and Holmgren A (2006) Inhibition of thioredoxin and thioredoxin reductase by 4-hydroxy-2-nonenal in vitro and in vivo. *J Am Chem Soc* **128**(6):1879-1885.

Go YM, Halvey PJ, Hansen JM, Reed M, Pohl J and Jones DP (2007) Reactive aldehyde modification of thioredoxin-1 activates early steps of inflammation and cell adhesion. *Am J Pathol* **171**(5):1670-1681.

Grattagliano I, Caraceni P, Calamita G, Ferri D, Gargano I, Palasciano G and Portincasa P (2008) Severe liver steatosis correlates with nitrosative and oxidative stress in rats. *Eur J Clin Invest* **38**(7):523-530.

Grimsrud PA, Picklo MJ, Sr., Griffin TJ and Bernlohr DA (2007) Carbonylation of adipose proteins in obesity and insulin resistance: identification of adipocyte fatty acid-binding protein as a cellular target of 4-hydroxynonenal. *Mol Cell Proteomics* **6**(4):624-637.

Hartley DP and Petersen DR (1997) Co-metabolism of ethanol, ethanol-derived acetaldehyde, and 4-hydroxynonenal in isolated rat hepatocytes. *Alcohol Clin Exp Res* **21**(2):298-304.

Hartley DP, Ruth JA and Petersen DR (1995) The hepatocellular metabolism of 4-hydroxynonenal by alcohol dehydrogenase, aldehyde dehydrogenase, and glutathione S-transferase. *Arch Biochem Biophys* **316**(1):197-205.

He L, Hou X, Kanel G, Zeng N, Galicia V, Wang Y, Yang J, Wu H, Birnbaum MJ and Stiles BL (2010) The critical role of AKT2 in hepatic steatosis induced by PTEN loss. *Am J Pathol* **176**(5):2302-2308.

Horie Y, Suzuki A, Kataoka E, Sasaki T, Hamada K, Sasaki J, Mizuno K, Hasegawa G, Kishimoto H, Iizuka M, Naito M, Enomoto K, Watanabe S, Mak TW and Nakano T (2004) Hepatocyte-specific Pten deficiency results in steatohepatitis and hepatocellular carcinomas. *J Clin Invest* **113**(12):1774-1783.

Molecular Pharmacology Fast Forward. Published on March 17, 2011 as DOI: 10.1124/mol.110.069534
This article has not been copyedited and formatted. The final version may differ from this version.

Leavens KF, Easton RM, Shulman GI, Previs SF and Birnbaum MJ (2009) Akt2 is required for hepatic lipid accumulation in models of insulin resistance. *Cell Metab* **10**(5):405-418.

Lee JO, Yang H, Georgescu MM, Di Cristofano A, Maehama T, Shi Y, Dixon JE, Pandolfi P and Pavletich NP (1999) Crystal structure of the PTEN tumor suppressor: implications for its phosphoinositide phosphatase activity and membrane association. *Cell* **99**(3):323-334.

Lee SR, Yang KS, Kwon J, Lee C, Jeong W and Rhee SG (2002) Reversible inactivation of the tumor suppressor PTEN by H2O2. *J Biol Chem* **277**(23):20336-20342.

Leslie NR, Bennett D, Lindsay YE, Stewart H, Gray A and Downes CP (2003) Redox regulation of PI 3-kinase signalling via inactivation of PTEN. *Embo J* **22**(20):5501-5510.

Liao Y and Hung MC (2010) Physiological regulation of Akt activity and stability. *Am J Transl Res* **2**(1):19-42.

Liu W, Akhand AA, Takeda K, Kawamoto Y, Itoigawa M, Kato M, Suzuki H, Ishikawa N and Nakashima I (2003) Protein phosphatase 2A-linked and -unlinked caspase-dependent pathways for downregulation of Akt kinase triggered by 4-hydroxynonenal. *Cell Death Differ* **10**(7):772-781.

Marshall AJ, Krahn AK, Ma K, Duronio V and Hou S (2002) TAPP1 and TAPP2 are targets of phosphatidylinositol 3-kinase signaling in B cells: sustained plasma membrane recruitment triggered by the B-cell antigen receptor. *Mol Cell Biol* **22**(15):5479-5491.

McMillian MK, Grant ER, Zhong Z, Parker JB, Li L, Zivin RA, Burczynski ME and Johnson MD (2001) Nile Red binding to HepG2 cells: an improved assay for in vitro studies of hepatosteatosis. *In Vitr Mol Toxicol* **14**(3):177-190.

Ozeki M, Miyagawa-Hayashino A, Akatsuka S, Shirase T, Lee WH, Uchida K and Toyokuni S (2005) Susceptibility of actin to modification by 4-hydroxy-2-nonenal. *J Chromatogr B Analyt Technol Biomed Life Sci* **827**(1):119-126.

Paradis V, Kollinger M, Fabre M, Holstege A, Poynard T and Bedossa P (1997) In situ detection of lipid peroxidation by-products in chronic liver diseases. *Hepatology* **26**(1):135-142.

Poli G, Schaur RJ, Siems WG and Leonarduzzi G (2008) 4-hydroxynonenal: a membrane lipid oxidation product of medicinal interest. *Med Res Rev* **28**(4):569-631.

Raza H and John A (2006) 4-hydroxynonenal induces mitochondrial oxidative stress, apoptosis and expression of glutathione S-transferase A4-4 and cytochrome P450 2E1 in PC12 cells. *Toxicol Appl Pharmacol* **216**(2):309-318.

Roede JR, Stewart BJ and Petersen DR (2008) Decreased expression of peroxiredoxin 6 in a mouse model of ethanol consumption. *Free Radic Biol Med* **45**(11):1551-1558.

Seki S, Kitada T, Yamada T, Sakaguchi H, Nakatani K and Wakasa K (2002) In situ detection of lipid peroxidation and oxidative DNA damage in non-alcoholic fatty liver diseases. *J Hepatol* **37**(1):56-62.

Shan X, Czar MJ, Bunnell SC, Liu P, Liu Y, Schwartzberg PL and Wange RL (2000) Deficiency of PTEN in Jurkat T cells causes constitutive localization of Itk to the plasma membrane and hyperresponsiveness to CD3 stimulation. *Mol Cell Biol* **20**(18):6945-6957.

Molecular Pharmacology Fast Forward. Published on March 17, 2011 as DOI: 10.1124/mol.110.069534
This article has not been copyedited and formatted. The final version may differ from this version.

Sorrentino P, Terracciano L, D'Angelo S, Ferbo U, Bracigliano A, Tarantino L, Perrella A, Perrella O, De Chiara G, Panico L, De Stefano N, Lepore M and Vecchione R (2010) Oxidative stress and steatosis are cofactors of liver injury in primary biliary cirrhosis. *J Gastroenterol*.

Stewart BJ, Doorn JA and Petersen DR (2007) Residue-specific adduction of tubulin by 4-hydroxynonenal and 4-oxononenal causes cross-linking and inhibits polymerization. *Chem Res Toxicol* **20**(8):1111-1119.

Stewart BJ, Roede JR, Doorn JA and Petersen DR (2009) Lipid aldehyde-mediated cross-linking of apolipoprotein B-100 inhibits secretion from HepG2 cells. *Biochim Biophys Acta*.

Tjalkens RB, Cook LW and Petersen DR (1999) Formation and export of the glutathione conjugate of 4-hydroxy-2, 3-E-nonenal (4-HNE) in hepatoma cells. *Arch Biochem Biophys* **361**(1):113-119.

Tsukamoto H, Horne W, Kamimura S, Niemela O, Parkkila S, Yla-Herttuala S and Brittenham GM (1995) Experimental liver cirrhosis induced by alcohol and iron. *J Clin Invest* **96**(1):620-630.

Vazquez F, Grossman SR, Takahashi Y, Rokas MV, Nakamura N and Sellers WR (2001) Phosphorylation of the PTEN tail acts as an inhibitory switch by preventing its recruitment into a protein complex. *J Biol Chem* **276**(52):48627-48630.

Watanabe S, Horie Y and Suzuki A (2005) Hepatocyte-specific Pten-deficient mice as a novel model for nonalcoholic steatohepatitis and hepatocellular carcinoma. *Hepatol Res* **33**(2):161-166.

Wullschleger S, Wasserman DH, Gray A, Sakamoto K and Alessi DR (2011) Role of TAPP1 and TAPP2 adaptors binding to PtdIns(3,4)P2 in regulating insulin sensitivity defined by knock-in analysis. *Biochem J*.

Yu CX, Li S and Whorton AR (2005) Redox regulation of PTEN by S-nitrosothiols. *Mol Pharmacol* **68**(3):847-854.

Molecular Pharmacology Fast Forward. Published on March 17, 2011 as DOI: 10.1124/mol.110.069534
This article has not been copyedited and formatted. The final version may differ from this version.

Footnotes

This work was supported by National Institutes of Health Institutes of Alcohol Abuse and Alcoholism grants [R37AA009300-14, 1-F32AA018613-01A1 and 1-F31AA018898-01].

Molecular Pharmacology Fast Forward. Published on March 17, 2011 as DOI: 10.1124/mol.110.069534
This article has not been copyedited and formatted. The final version may differ from this version.

Figure Captions

Scheme 1. Proposed working model for 4-HNE mediated Akt activation in hepatocytes. Following exposure to 4-HNE, Akt is phosphorylated due to 4-HNE mediated PTEN inhibition. This contributes to increased levels of lipid accumulation and cell survival.

Figure 1. Time course and dose dependency of 4-HNE induced Akt phosphorylation. HepG2 cells were washed twice in serum free media and treated with: (A) Increasing concentrations of 4-HNE in serum free media for 1 hour or (B) With 100μM 4-HNE from 5-120 min in serum free media. Cells were lysed, run on an 8% SDS PAGE, blotted and probed for p-Ser473 Akt, p-Thr308Akt, total Akt and actin. (C) Densitometric analysis of p-Ser473Akt/Akt/Actin. Blots are representative of at least 3 independent experiments, **p<0.001.

Figure 2. Fluorescence measurements of intracellular ROS generation following 4-HNE addition. Relative rate of ROS generation (DCF production/min) following the addition of increasing concentrations of 4-HNE in serum free media for 2hr. HepG2 cells were incubated in triplicate with increasing concentrations of 4-HNE (0-250μM) or 1mM H_2O_2 in the presence of 10μg/ml 2', 7'-dichlorofluorescein diacetate at 37^{o}C. **p<0.01.

Figure 3. Characterization of 4-HNE mediated PtdIns (3,4,5) P_3 production in HepG2 cells. (A) Quantification of PtdIns (3,4,5) P_3 using TR-FRET. Cells were treated with or without 100μM 4-HNE (60 min) in serum-free media. Cells were lysed and PtdIns (3,4,5) P_3 extracted and quantified as per methods. All samples were performed in triplicate. ***p<0.001 (B) Immunofluorescent staining of control, 100μM 4-HNE (60 min) and 100nM insulin (15min) treated HepG2 cells with mouse-monoclonal anti-PtdIns (3,4,5) P_3 and an anti-mouse secondary antibody conjugated to Texas Red (Red= PtdIns (3,4,5) P_3, Blue= Hoechst 33342 nuclear

Molecular Pharmacology Fast Forward. Published on March 17, 2011 as DOI: 10.1124/mol.110.069534
This article has not been copyedited and formatted. The final version may differ from this version.

staining). (C) Confocal microcopy of eGFP-TAPP1 transfected HepG2 cells stimulated with 100μM 4-HNE (60 min) and 100nM insulin (15min) (Green=eGFP-TAPP1, Blue= Hoechst 33342 nuclear staining).

Figure 4. Effect of Ly294002 and okadaic acid on 4-HNE induced Akt phosphorylation. (A) Increased phosphorylation of Akt is PI3K-dependent but not PP2A dependent. Cells were treated in serum free media with 100μM 4-HNE or control for 60 min following pre-incubation with (A) Ly294002 (50μM 60 min) or (B) Okadaic acid (100nM 30 min). After treatment, cells were lysed and Western blotted for phosphorylation of Akt on Ser473 (Ly294002) or Thr308 (okadaic acid). (C) Densitometric analysis of p-Thr308Akt/total Akt/Actin from Western blots presented in Figure 4B. (D) Densitometric analysis of the blots presented in Figure 4B. Okadaic acid samples represented as percent control (non-okadaic acid compared to okadaic acid). Western blots were quantified using ImageJ (NIH Freeware) and analyzed using 1-way-ANOVA and GraphPad. **p<0.01, ***p<.001.

Figure 5. Effects of 4-HNE on PTEN phosphorylation and activity. (A) Phosphorylation state of PTEN, cells were treated in serum free media with 100μM 4-HNE or control for 0-2 hours. Following treatment, cells were lysed and 20μg of protein was loaded onto a 7% SDS PAGE gel as per methods. (B) PTEN activity is inhibited by 4-HNE in HepG2 cells. Cells were treated in serum free media with 25,100μM 4-HNE for 60 min or 1mM H_2O_2 for 10 min, lysed and PTEN activity was measured using a malachite green phosphate release assay and DiC_8 PtdIns(3,4,5)P_3. All samples were performed in triplicate. ** p<0.01.

Figure 6. Biotin hydrazide modification and examination of PTEN in 4-HNE treated HepG2 cells. (A) Streptavidin pulldown of 4-HNE modified PTEN from HepG2 cells. 125 μg of

Molecular Pharmacology Fast Forward. Published on March 17, 2011 as DOI: 10.1124/mol.110.069534
This article has not been copyedited and formatted. The final version may differ from this version.

protein from 4-HNE treated (100μM/60 min in serum free media) or untreated cells was incubated for 2 h with 2.5 mM biotin hydrazide and purified using streptavidin pulldown. Samples were subsequently analyzed using SDS PAGE/Western blotting with rabbit polyclonal anti-PTEN. All samples were performed in triplicate. (B) Densitometric analysis of Western blots *** $p<0.001$.

Figure 7. Effects of 4-HNE on recombinant PTEN. (A) Western Blotting of rPTEN treated with increasing molar ratios of 4-HNE. Purified PTEN was incubated with increasing molar ratios of 4-HNE for 30 min at room temperature. Samples were boiled in 5X SDS loading buffer, run on an 8% SDS PAGE gel, blotted and probed for 4-HNE using anti-4-HNE polyclonal antibodies. Blots were stripped and reprobed for PTEN. (B) Inhibition of rPTEN by 4-HNE treatment. Purified rPTEN was incubated with increasing molar ratios of 4-HNE and phosphate release activity assays performed using PtdIns $(3,4,5)P_3$ DiC8 as a substrate as per methods. The data presented were derived from three independent experiments. Statistical analysis was via 1-way analysis of variance *$p<0.05$, **$p<0.01$.

Figure 8. Figure 8. MS analysis of unmodified and 4-HNE modified rPTEN. The mass spectra obtained for (A) control and (B) 4-HNE treated rPTEN details a mass shift of 156 Da in the treated intact protein, corresponding with a mass addition of a 4-HNE Michael-type adduct. The unmodified protein displays an isotopic mass average of 51,209 m/z, with a resolution of 58 and signal-to-noise ratio of 358. The 4-HNE modified protein has an observed m/z of 51,365 kDa, with a resolution of 55 and signal-to-noise ratio of 410. While this mass shift indicates one predominant 4-HNE adduct, given the expected instrument resolution at this m/z, the presence of native PTEN and PTEN with multiple 4-HNE modifications is likely.

Molecular Pharmacology Fast Forward. Published on March 17, 2011 as DOI: 10.1124/mol.110.069534
This article has not been copyedited and formatted. The final version may differ from this version.

Figure 9. Effect of 4-HNE addition on lipid accumulation in HepG2 cells. (A) 4-HNE neutral lipid effects at 1 h treatment followed by 24 h recovery. (B) Nile red staining for lipid with 1 h treatment and 24 h recovery. Blue = DAPI nuclear staining, Red = Nile red lipid staining. (C) Neutral Lipid effects of specific pathway disruptors or oleate. ** $p < 0.01$, *** $p < 0.001$.

Figure 10. Dose-dependency of 4-HNE on Akt phosphorylation in primary rat hepatocytes. Freshly isolated primary rat hepatocytes were treated with increasing concentrations of 4-HNE (0-100μM) for 1 hour in serum free media. As a positive control for Akt phosphorylation, 1mM H_2O_2 (5 min) was used. (A) Cells were lysed, run on an 8% SDS PAGE, Western blotted and probed for p-Ser473 Akt, total Akt and actin. (B) Quantification of Western blots presented in Figure 10A. N=4, *$p<0.05$, **$p<0.01$.

Scheme 1.

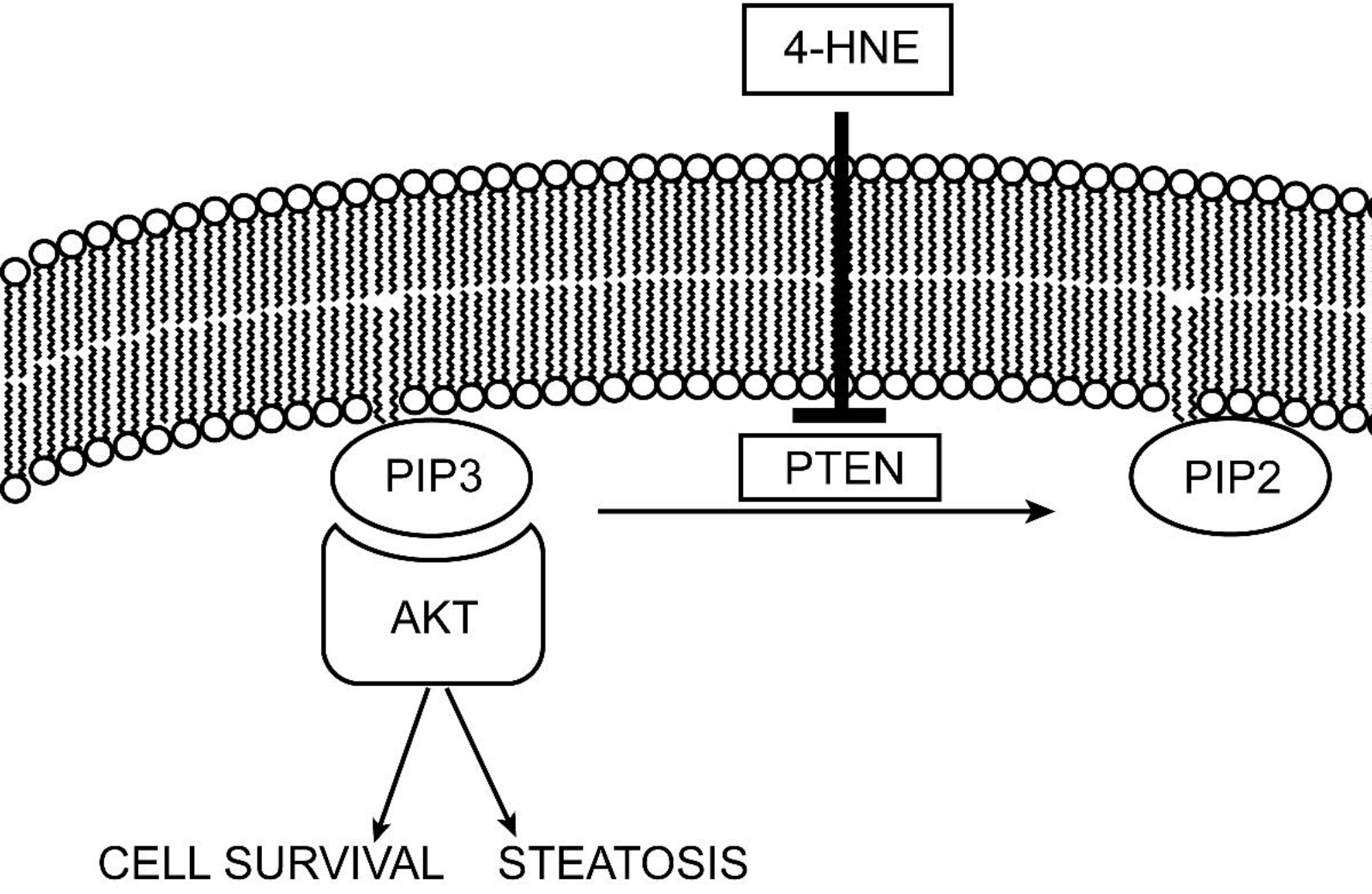

Figure 1A.

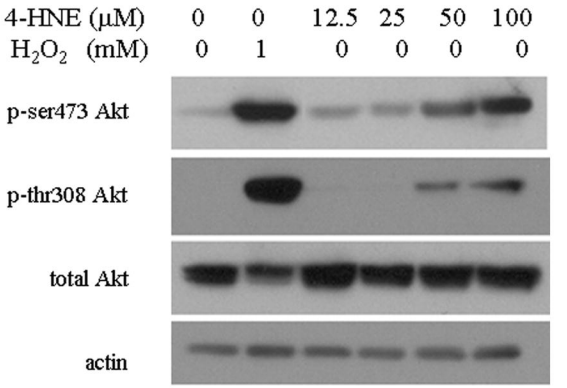

Figure 1B.

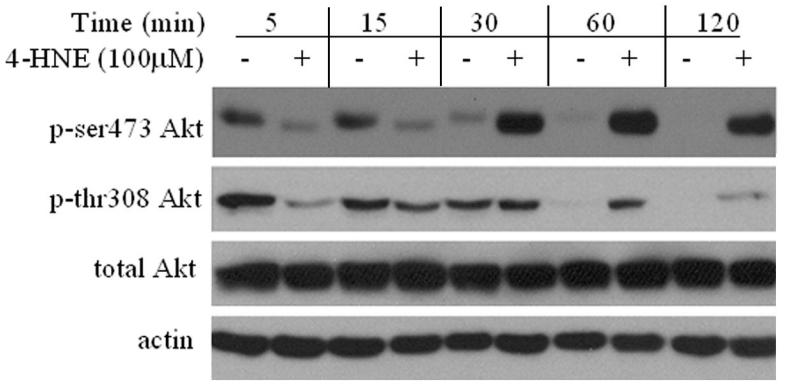

Figure 1C.

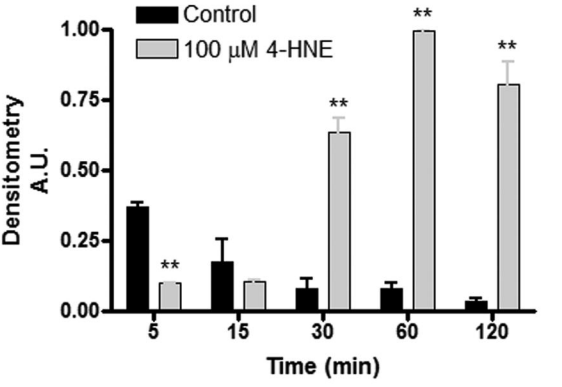

Figure 2.

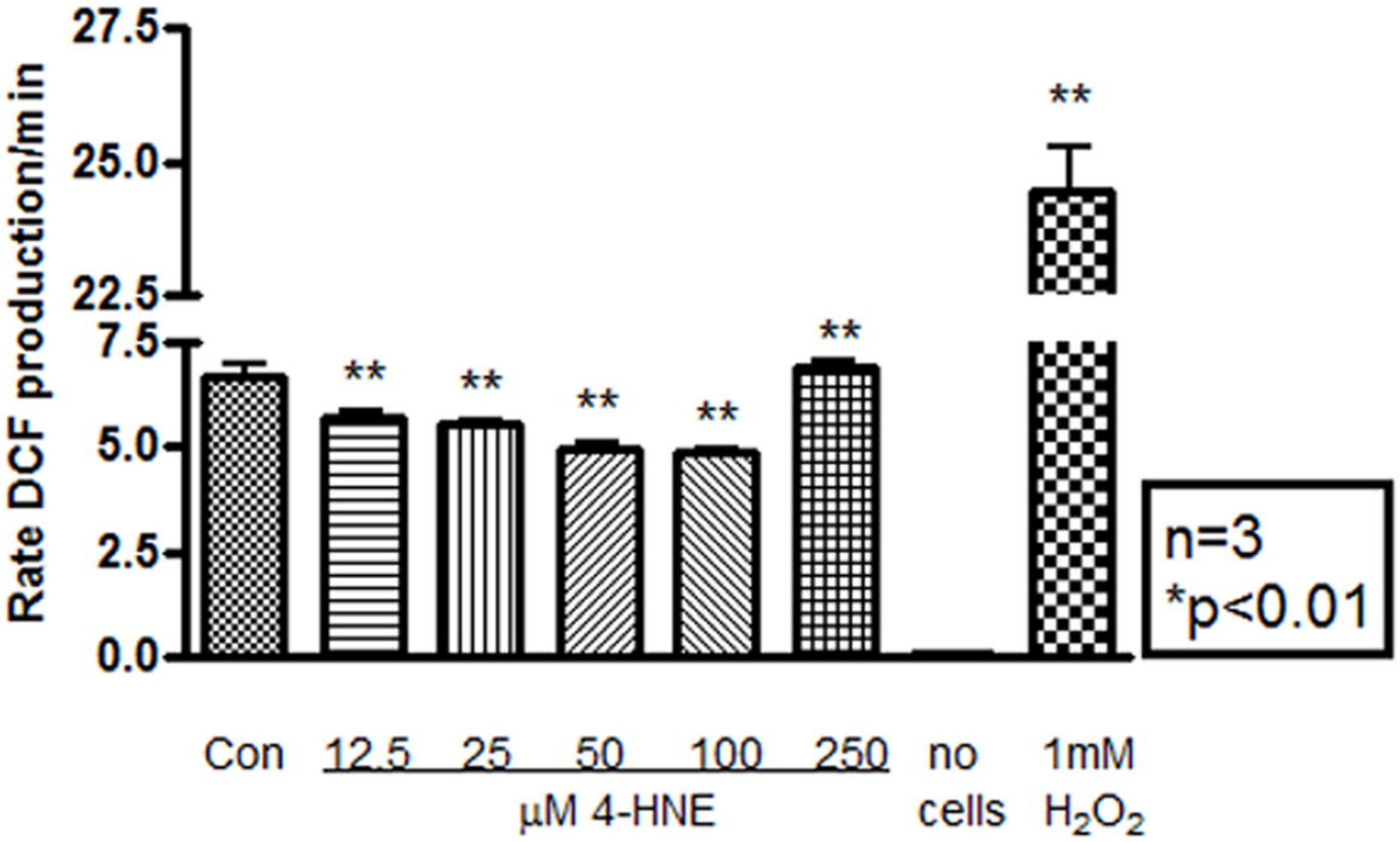
Rate DCF production/min
27.5
25.0
22.5
7.5
5.0
2.5
0.0
**
**
**
**
**
**
n=3
*p<0.01
Con
12.5
25
50
100
250
no cells
1mM H2O2
μM 4-HNE

Figure 3A.

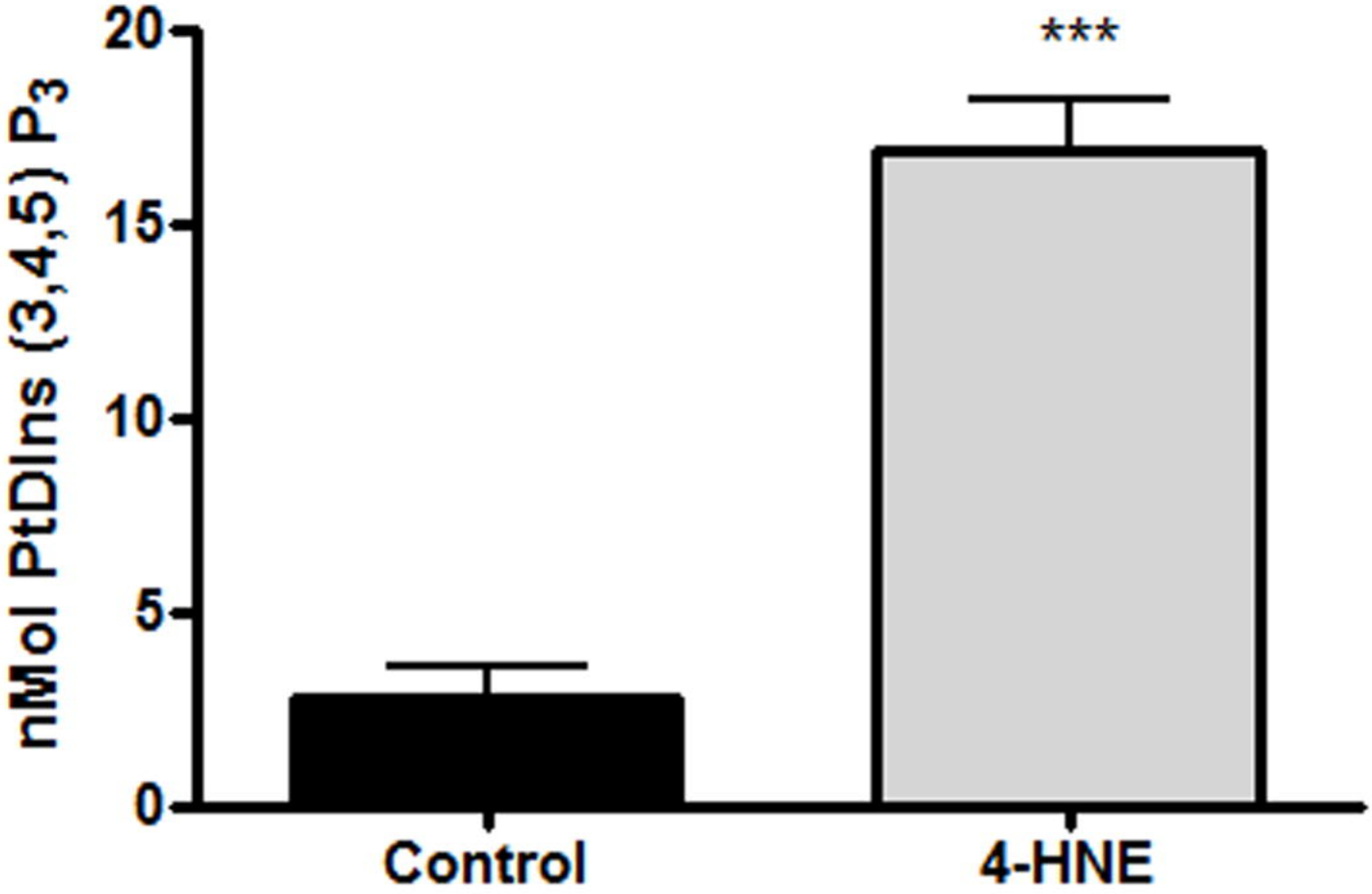

Figure 3B.

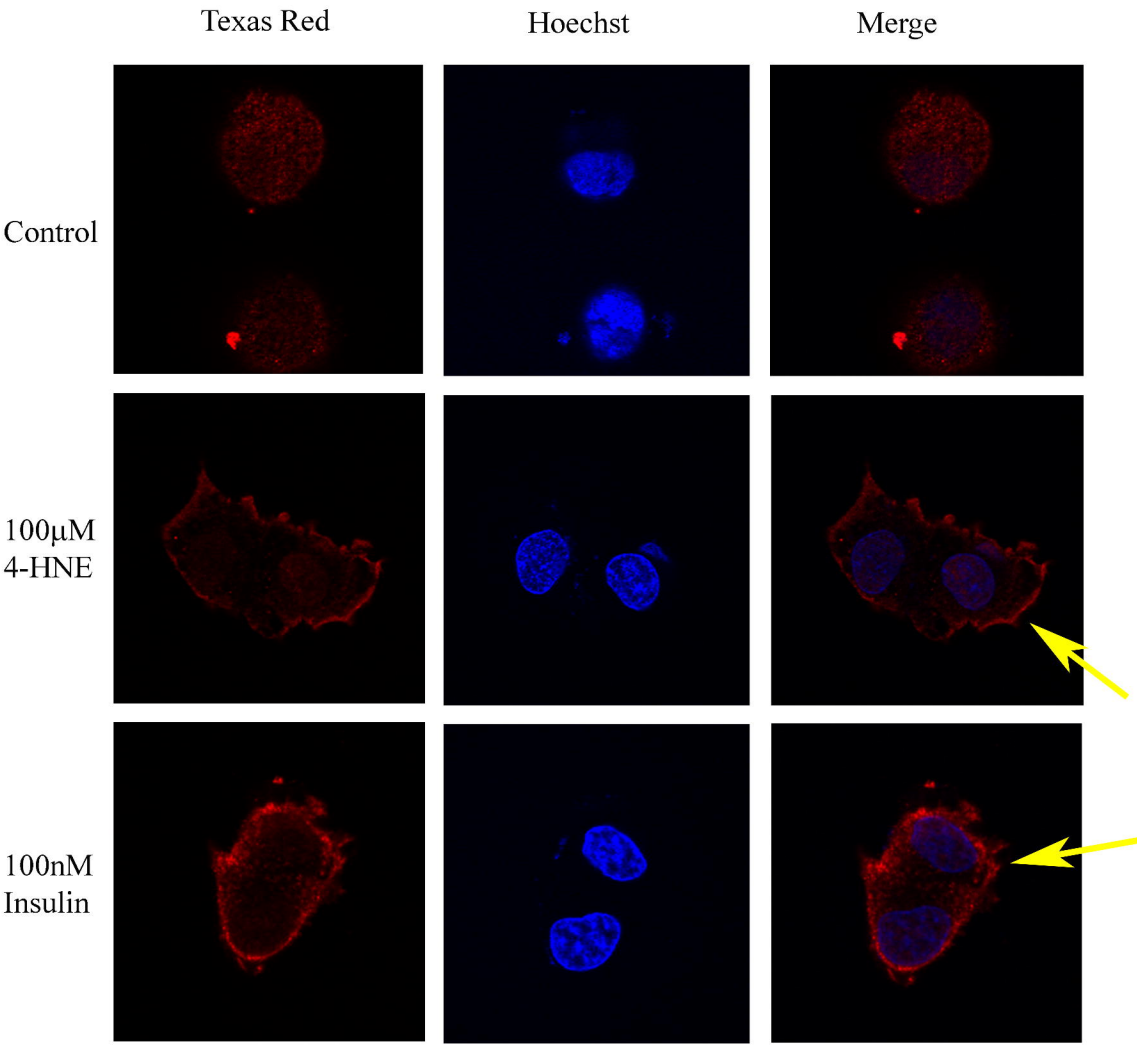

Figure 3C.

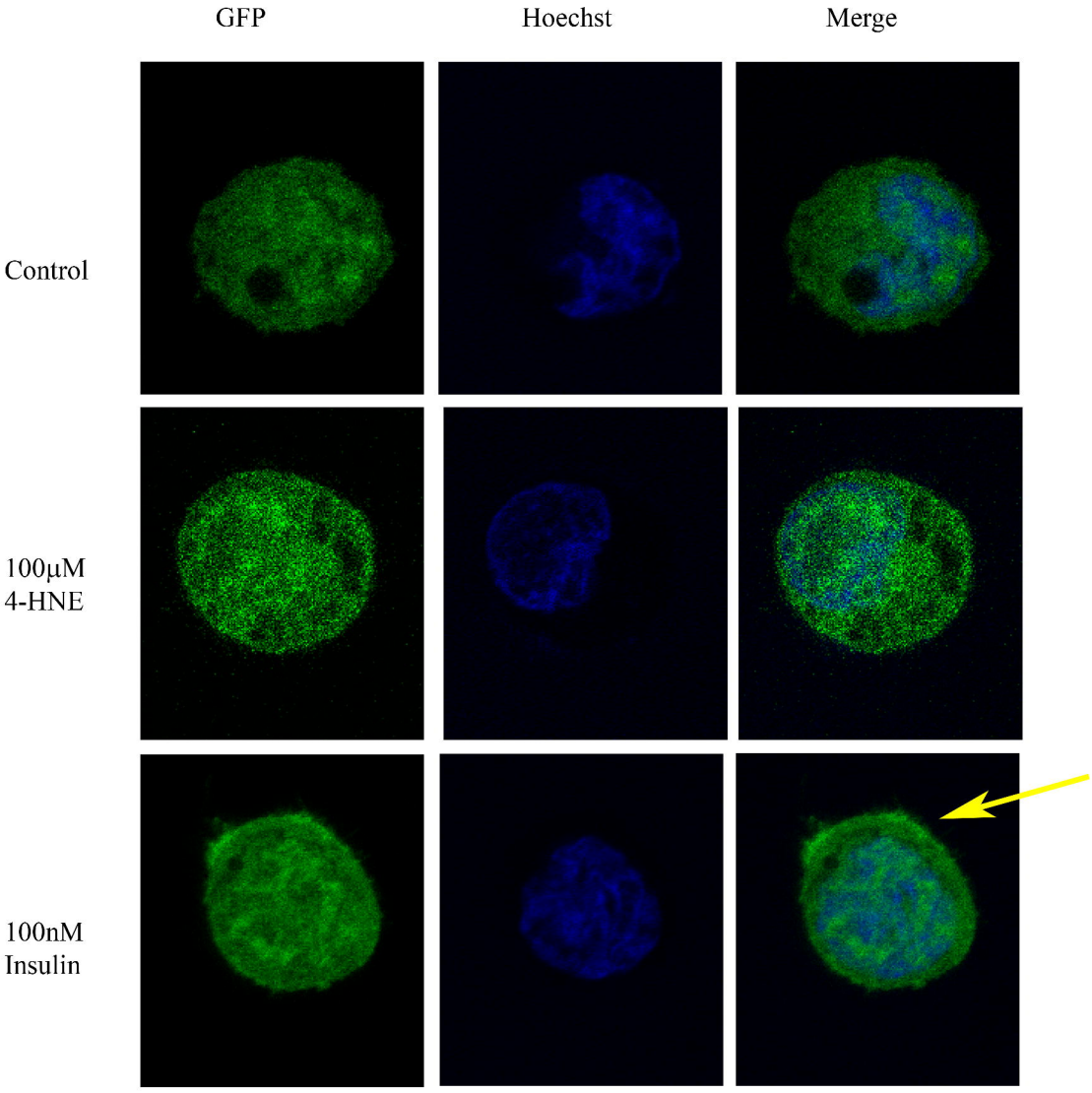

Figure 4A.

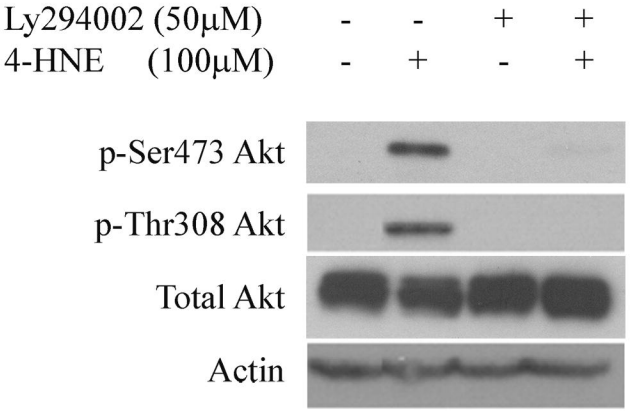

Figure 4B.

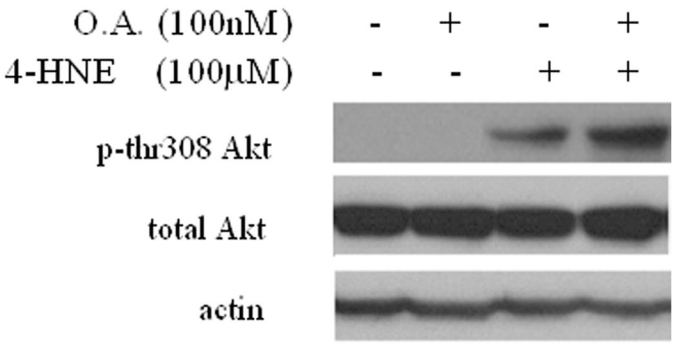

Figure 4C.

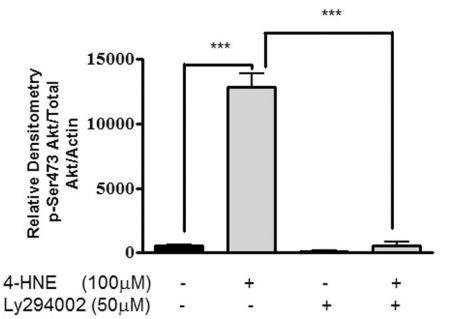

Figure 4D.

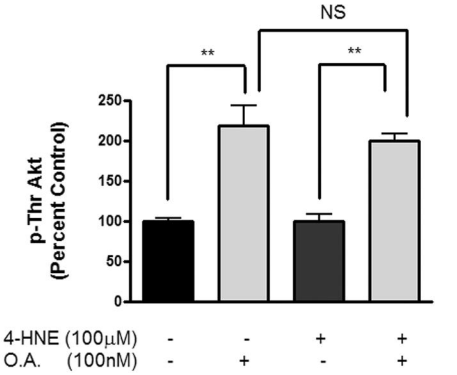

Figure 5A.

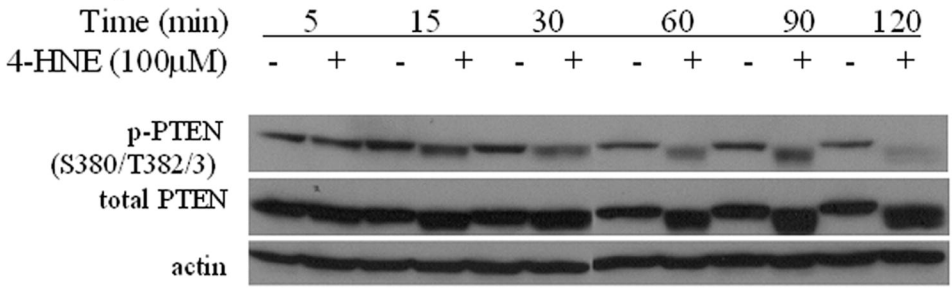

Figure 5B.

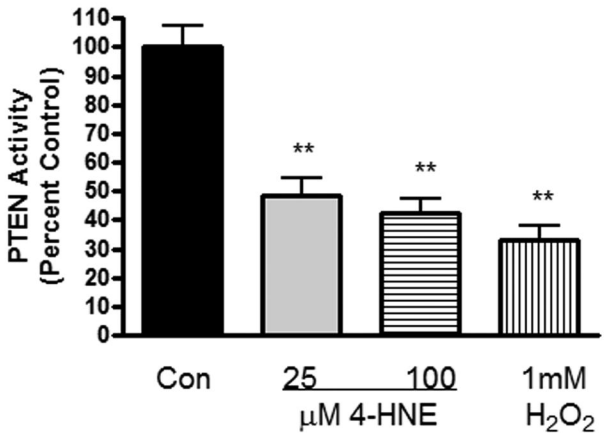

Figure 6A.

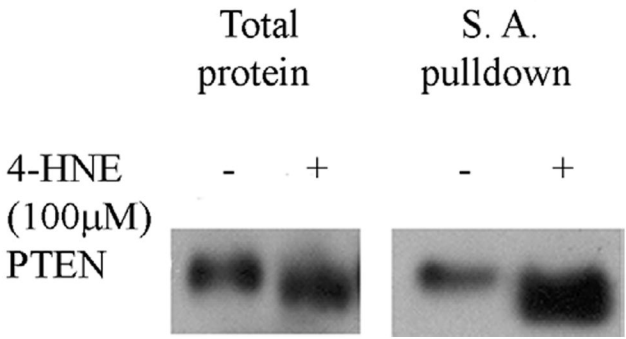

Figure 6B.

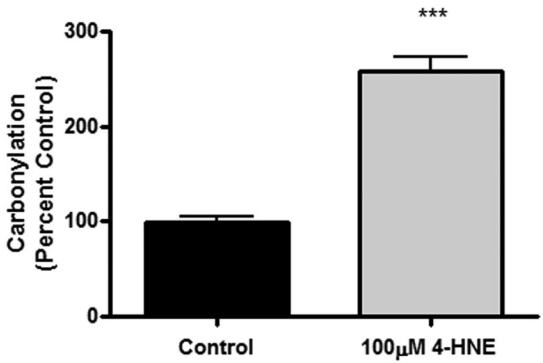

Figure 7A.

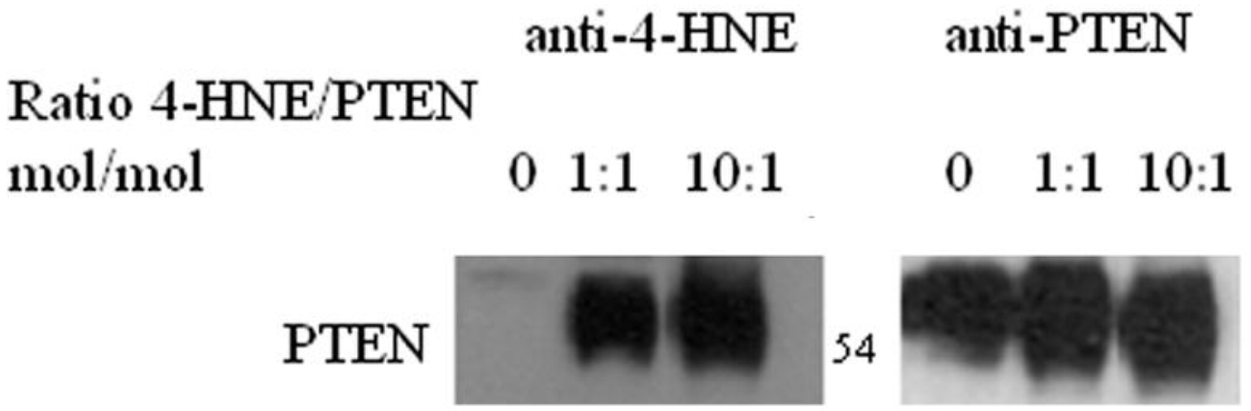

Figure 7B.

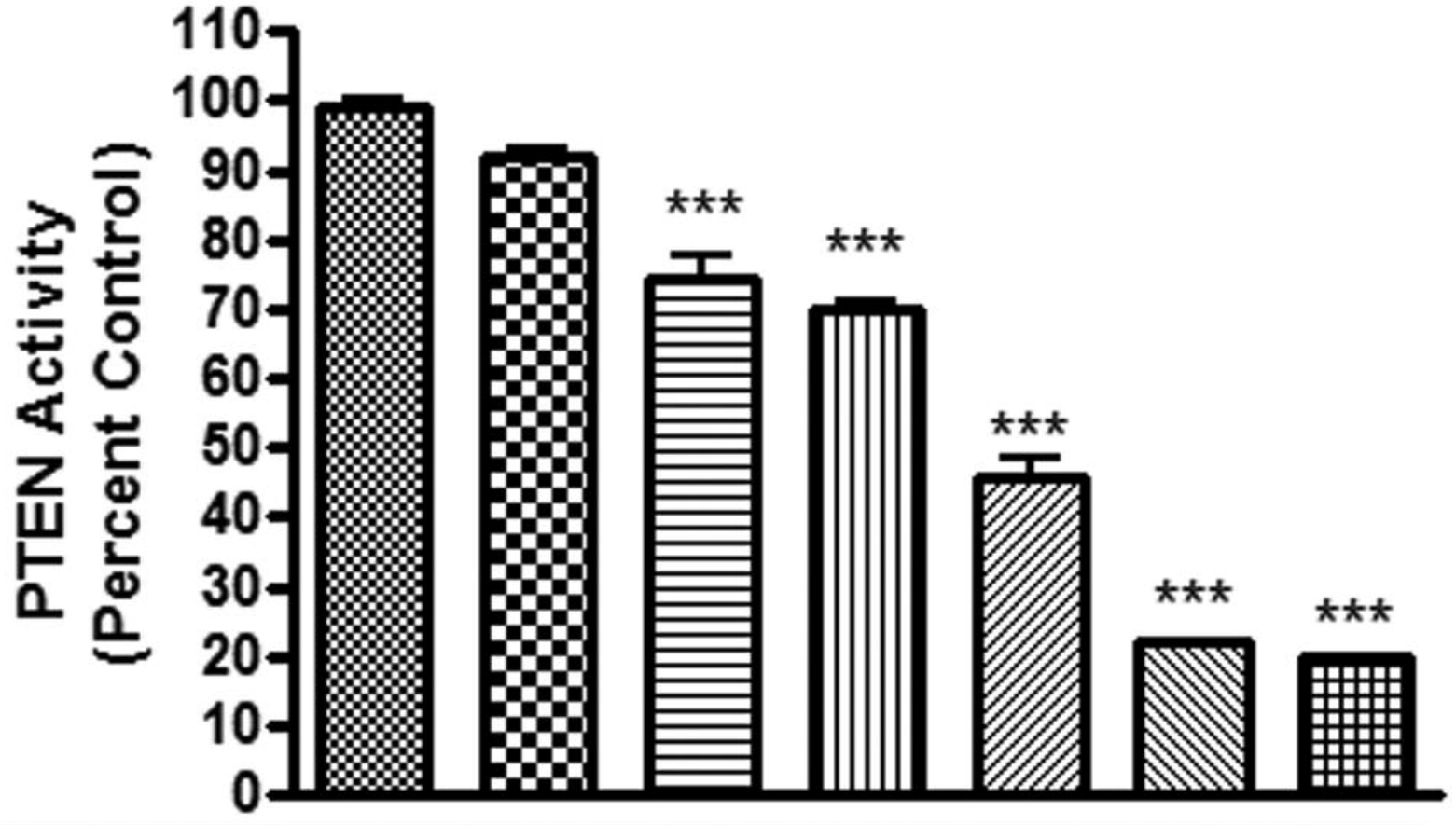

4-HNE (μM)	0	0.025	0.25	1.0	2.0	5.0	10.0
4-HNE:PTEN mol:mol	0	0.1:1	1:1	2.5:1	5:1	10:1	20:1

Figure 8

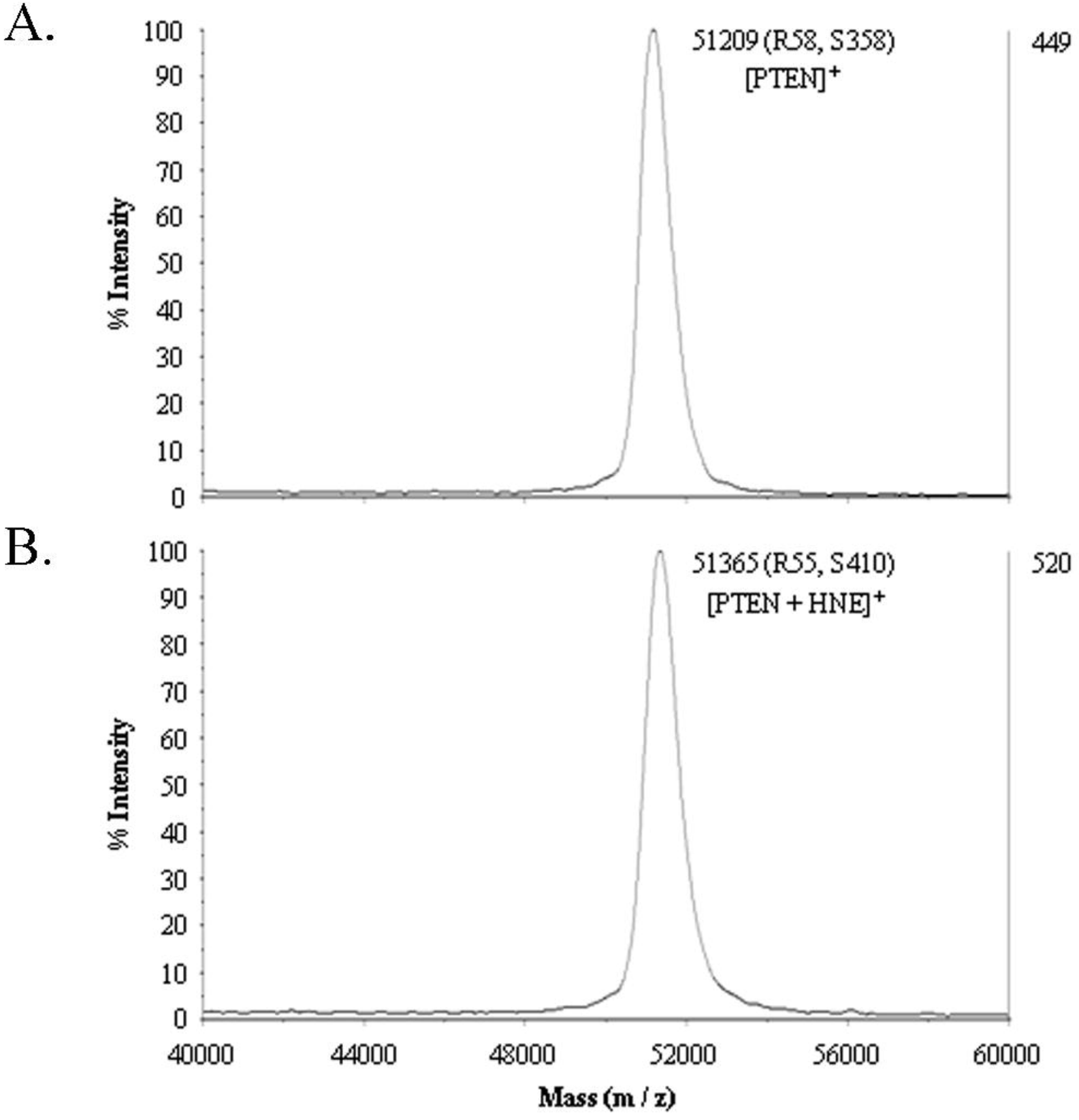
A.
100
90
80
70
60
50
40
30
20
10
0
% Intensity
51209 (R58, S358)
[PTEN]+
449
B.
100
90
80
70
60
50
40
30
20
10
0
% Intensity
51365 (R55, S410)
[PTEN + HNE]+
520
40000
44000
48000
52000
56000
60000
Mass (m / z)

Figure 9A.

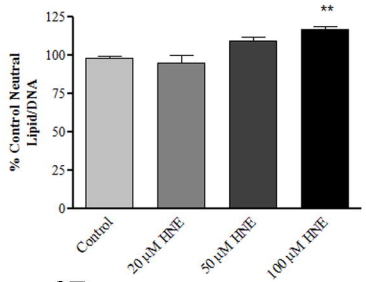

Figure 9B.

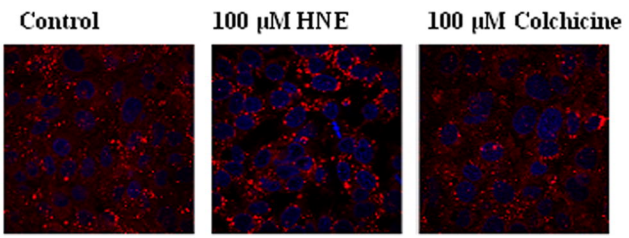

Figure 9C.

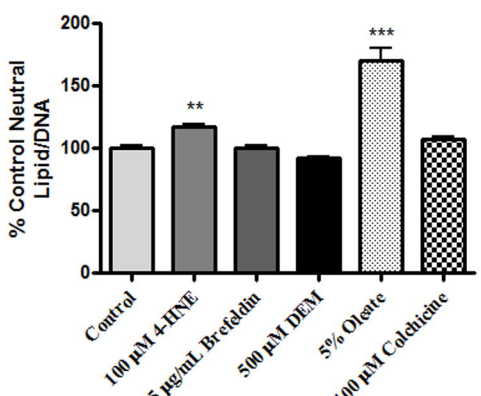

Figure 10A.

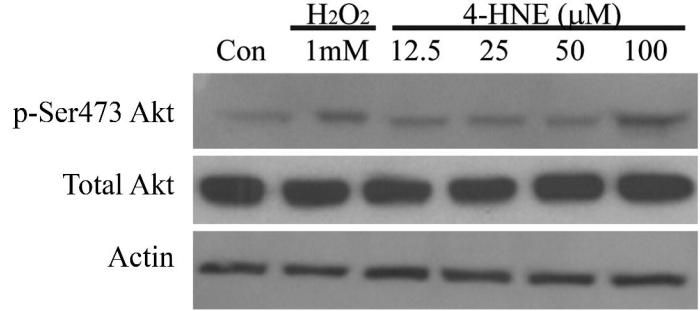

Figure 10B.